BRNO UNIVERSITY OF TECHNOLOGY
VYSOKÉ UČENÍ TECHNICKÉ V BRNĚ

FACULTY OF CHEMISTRY
FAKULTA CHEMICKÁ

INSTITUTE OF MATERIALS SCIENCE
ÚSTAV CHEMIE MATERIÁLŮ

EVALUATION OF THE QUALITY OF COLLAGEN SAMPLES IN SOLID PHASE USING CIRCULAR DICHROISM

HODNOCENÍ KVALITY KOLAGENOVÝCH VZORKŮ V PEVNÉ FÁZI POMOCÍ CIRKULÁRNÍHO DICHROISMU

MASTER'S THESIS
DIPLOMOVÁ PRÁCE

AUTHOR
AUTOR PRÁCE
Bc. Matej Ďubašák

SUPERVISOR
VEDOUCÍ PRÁCE
doc. Ing. Lucy Vojtová, Ph.D.

BRNO 2018

Zadání diplomové práce

Číslo práce:	FCH-DIP1170/2017
Ústav:	Ústav chemie materiálů
Student:	**Bc. Matej Ďubašák**
Studijní program:	Chemie, technologie a vlastnosti materiálů
Studijní obor:	Chemie, technologie a vlastnosti materiálů
Vedoucí práce:	**doc. Ing. Lucy Vojtová, Ph.D.**
Akademický rok:	2017/18

Název diplomové práce:

Hodnocení kvality kolagenových vzorků v pevné fázi pomocí cirkulárního dichroismu

Zadání diplomové práce:

1. Lit. rešerše – kolagen a charakterizace jeho sekundární struktury
2. Příprava kolagen/želatinových filmů, optimalizace metody CD
3. Testování různých kolagenových vzorků
4. Vyhodnocení a diskuze
5. Závěr

Termín odevzdání diplomové práce: 7.5.2018

Diplomová práce se odevzdává v děkanem stanoveném počtu exemplářů na sekretariát ústavu. Toto zadání je součástí diplomové práce.

-- -- -- -- -- -- -- -- -- -- --	-- -- -- -- -- -- -- -- -- -- --	-- -- -- -- -- -- -- -- -- -- --
Bc. Matej Ďubašák	doc. Ing. Lucy Vojtová, Ph.D.	prof. RNDr. Josef Jančář, CSc.
student(ka)	vedoucí práce	vedoucí ústavu
		-- -- -- -- -- -- -- -- -- -- --
V Brně dne 31.1.2018		prof. Ing. Martin Weiter, Ph.D.
		děkan

ABSTRACT

The diploma thesis deals with the novel qualitative analysis of collagen films by circular dichroism in solid phase. Theoretical part describes collagen and its secondary structure, spectroscopic methods of circular dichroism (CD) and attenuated total reflectance (ATR).

The experimental part deals with the preparation of homogeneous and transparent collagen films, the volume, concentration and method of drying optimization. Subsequently, a calibration line with different ratios of collagen and gelatine was measured and evaluated. Obtained linear regression equation was used to determine the content of collagen in the modified samples. The results of evaluated modified samples were compared with ATR spectroscopy measurements. ATR measurements showed higher content of collagen than CD measurements. Samples with the lowest and the highest contents of collagen are same for both methods. It proves that we can compare samples with different collagen content to each other but we cannot determine exact collagen content by connecting these two methods.

The optimized method of CD can be used to prepare and measure the exact content of collagen in the samples especially within collagen production to reach the constant quality of collagen at each step of fabrication.

KEYWORDS

Collagen, gelatine, circular dichroism, infrared spectroscopy

ABSTRAKT

Diplomová práca sa zaoberá novou kvalitatívnou analýzou kolagénových vrstiev pomocou cirkulárneho dichroizmu v pevnej fáze. Teoretická časť opisuje kolagén a jeho sekundárnu štruktúru, spektroskopické metódy cirkulárneho dichroizmu (CD) a zoslabenej úplnej reflektancie (ATR).

Experimentálna časť sa zaoberá prípravou homogénnych a transparentných kolagénových filmov a optimalizáciou objemu, koncentrácie a sušenia. Následne sa zmerala a vyhodnotila kalibračná krivka s rôznymi pomermi kolagénu a želatíny. Získaná rovnica lineárnej regresie sa použila na stanovenie obsahu kolagénu v modifikovaných vzorkách. Výsledky hodnotených modifikovaných vzoriek boli porovnané s meraniami ATR spektroskopie. Merania ATR ukázali vyšší obsah kolagénu ako CD merania. Vzorky s najnižším a najvyšším obsahom kolagénu sú pre obe metódy rovnaké. Dokazuje to, že môžme porovnávať vzorky s rôznym obsahom kolagénu navzájom, ale nemôžeme určiť presný obsah kolagénu pripojením týchto dvoch metód.

Optimalizovaná metóda CD sa môže použiť na prípravu a meranie presného obsahu kolagénu vo vzorkách, najmä v rámci výroby kolagénu, aby sa dosiahla konštantná kvalita kolagénu v každom kroku výroby.

KLÍČOVÉ SLOVÁ

Kolagén, želatina, cirkulárny dichroizmus, infračervená spektroskopia

QUOTATION

ĎUBAŠÁK, M. *Hodnocení kvality kolagenových vzorků v pevné fázi pomocí cirkulárního dichroismu*. Brno: Vysoké učení technické v Brně, Fakulta chemická, 2018. 68 s. Vedoucí diplomové práce doc. Ing. Lucy Vojtová, Ph.D.

DECLARATION

I declare that the diploma thesis has been worked out by myself and that all the quotations from the used literary sources are accurate and complete. The content of the diploma thesis is the property of the Faculty of Chemistry of Brno University of Technology and all commercial uses are allowed only if approved by both the supervisor and the dean of the Faculty of Chemistry, BUT.

.....
student's signature

AKNOWLEDGMENTS

I would like to thank my advisor M. S. Johana Babrnáková for valuable advises and creation of the good work conditions, my supervisor Assoc. Prof. LucyVojtová for helpful discussions, interest and English correction and all colleagues involved in this work. I would like to thank also my all family and mainly my girlfriend Andrea for supporting me and helping me in every moment I need it. This work was supported by the CEITEC 2020 (LQ1601) with financial support from the Ministry of Education, Youth and Sports of the Czech Republic under the National Sustainability Programme II.

CONTENT

1 INTRODUCTION

Collagens are abundant proteins in animals and present in all multicellular animals. Due to their helical fibrous domain consisting of three α peptide chains (α chains), collagens have unique and genetically conserved structures [1], [2]. So it has been widely applied in various fields, including biomedical materials, drug delivery vectors, tissue engineering applications and cosmetics [1], [3].

A variety of commercial collagen sources are used for tissue-engineering applications as well as for cell studies that require collagen matrices. These materials, often from poorly specified preparations, make comparisons between studies of various collagen materials difficult. An additional issue is that collagen source materials are often prepared differently in each laboratory, complicating further attempts at comparisons of biological outcomes [4].

Food or medical grade collagen product development requires careful quality control in order to maximize yields, purity and reproducibility. Different techniques are necessary to be used for characterization of different collagen forms of insoluble collagen particles of micron size (centrifugation, optical microscopy, rheology), through soluble collagen of nanometer scale (electrophoresis, TEM, CD spectroscopy) to subnanometer scale of peptides and gelatin (amino acid analysis, peptide mapping). Usually many methods needs to be used to get objective information, which gives objective view about the sample. Proposed CD spectroscopy method characterizes air dried insoluble collagen, soluble collagen and gelatin films.

Solid-state spectroscopy provides valuable informationon solid-state structure and supramolecular properties which are not obtainable from the solution phase. However, very few chirality measurements in the solid state have been reported to date. This is because measurement of chiroptical properties in the solid state using a commercially available circular dichroism CD spectrophotometer is extremely difficult [5].

One of the aims of presented diploma thesis is to summarize the characteristics of collagen and its structure. It is focused on optimization of collagen films preparation and characterization. The work explains problems and complications, which are connected with collagen and work with them. Followly collagen films were measured and analysed by circular dichroism (CD) and the best conditions for preparation of films were optimized. Based on the collagen/gelatine calibration curve, collagen samples with different preparation conditions measured by CD spectroscopy were compared with attenuated total reflectance (ATR) spectroscopy results.

2 THEORETICAL PART

2.1 Collagen

Collagen is the primary structural material of vertebrates and the most abundant mammalian protein accounting for approximately 30 % of total body proteins. Collagen is synthesized by fibroblasts, which usually originate from pluripotential adventitial cells or reticulum cells. It is present in tissues mainly because of its mechanical properties. Its biological plastic due to high tensile strength and minimal expressibility. It has alsohigh affinity to water. Collagen is relatively stable due to its function as the primary structural protein in the body, but it is still liable to collagenolytic degradation by enzymes. It is easily absorbable in the body and has very low antigenicity. Moreover, it is nontoxic, biocompatible and biodegradable. Biodegradability can be regulated by cross-linking [6], [7].Several distinct types of collagen had been identified, which collectively, represent about one third of the total protein of vertebrate animals. As a function of structure and supramolecular organization, they were grouped as fibril-forming (types I, II, III, V, XI), fibril-associated (types IX, XII, XIV), membrane (types IV, VII, VIII, X) or other specific function. Main types of collagen and their distribution in our tissues are shown in Tab. 1 [7].

Tab. 1: Chain composition and body distribution of collagen types [7].

Collagen type	Chain composition	Tissue distribution
I	$(\alpha 1(I))_2\alpha 2(I)$, trimer $(\alpha 1(I))_3$	Skin, tendon, bone, cornea, dentin, fibrocartilage, large vessels, intestine, uterus, dentin, dermis, tendon
II	$(\alpha 1(II))_3$	Hyaline cartilage, vitreous, nucleus pulposus, notochord
III	$(\alpha 1(III))_3$	Large vessels, uterine wall, dermis, intestine, heart valve, gingiva (usually coexists with type I except in bone, tendon, cornea)
IV	$(\alpha 1(IV))_2\alpha 2(IV)$	Basement membranes
V	$\alpha 1(V)\alpha 2(V)(3(V)$ or $(\alpha 1(V))_2\alpha 2(V)$ or $(\alpha 1(V))_3$	Cornea, placental membranes, bone, large vessels, hyaline cartilage, gingiva
VI	$\alpha 1(VI)\alpha 2(VI)\alpha 3(VI)$	Descemet's membrane, skin, nucleus pulposus, heart muscle
VII	$(\alpha 1(VII))_3$	Skin, placenta, lung, cartilage, cornea
VIII	$\alpha 1(VIII)$ $\alpha 2(VIII)$ chain organization of helix unknown	Produced by endothelial cells, Descemet's membrane
IX	$\alpha 1(IX)\alpha 2(IX)\alpha 3(IX)$	Cartilage
X	$(\alpha 1(X))_3$	Hypertrophic and mineralizing cartilage
XI	$1\alpha 2\alpha 3\alpha_1$ or $\alpha 1(XI)\alpha 2(XI)\alpha 3(XI)$	Cartilage, intervertebral disc, vitreous humour
XII	$(\alpha 1(XII))_3$	Chicken embryo tendon, bovine periodontal ligament
XIII	Unknown	Cetal skin, bone, intestinal mucosa

2.1.1 Collagen structure

The unique physiological and biomaterial characteristics of collagen compared with most synthetic polymers derive from the structural complexity of the collagen molecule. The various levels of order observed in collagen are illustrated inFig. 1. The collagen molecule consists of three polypeptide α-chains, each consisting of more than 1000 amino acids. They are twined around one another in right-handed directionwith a pitch of approximately 8.6 nm. Each chain has an individual twist in the left-handed directions. The principal feature that affects a helix formation is a high content of glycine (Gly) and amino acid residues.This particular structure, mainly stabilized by intra- and inter-chain hydrogen bonding between adjacent–CO and –NH groups, but also by covalent bonds, is

the product of an almost continuous repeating of the Gly-X-Y- sequence, where X is mostly proline (Pro) and Y is mostly hydroxiproline (Hyp). The basic collagen molecule is rod-shaped with a length and a width of about 300 nm and 1.5 nm. This extreme ratio of the dimensions gives rise to high viscosity in solutions and high mobility in electrical fields [6], [7], [8], [9], [10].

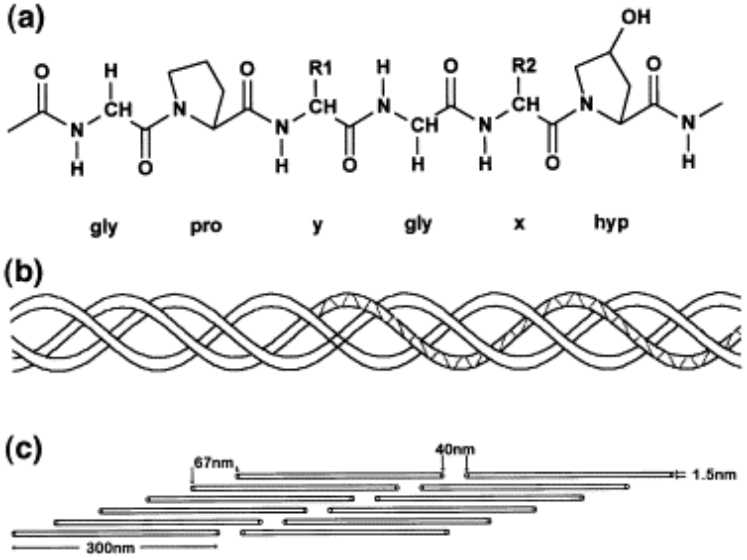

Fig. 1:Chemical structure of collagen type I. (a) Primary amino acid sequence, (b) secondary left handed helix and tertiary right handed triple-helix structure and (c) staggered quaternary structure [7].

A major stabilizing feature of α-helical and β-sheet protein structures is the participation of every backbone carbonyl and amide group in NH··O=C hydrogen bonds. Examination of the triple-helix shows a serious deficiency in this regard. In each Gly-X-Y tripeptide unitare sets of hydrogen bonds between the amide group of the Gly and carbonyl group of the residue in the X position in the adjacent chain of the triple-helix, (Gly)NH··O=C (X) (Fig. 2a). This leaves the carbonyl group of the Gly residues and the carbonyl of the residue in the Y position with no amide hydrogen bonding partners. If the X or Y positions are occupied by amino acids, rather than Pro or Hyp, then their amide groups are also available for hydrogen bonding, but no carbonyl in the triple helix is within bonding distance. In addition, the hydroxyl group of Hyp points out from the triple helix and cannot directly hydrogen bond to any other group within the molecule. The manner in which these groups are satisfied is seen in the Gly→Ala peptide structure, where an extensive and ordered water network forms hydrogen bonds with all available carbonyl and Hyp hydroxyl groups (Fig. 2). The structure also shows CαH··O=C bonds, which constitute a network of weak but systematic hydrogen bonds. All available groups of the peptide backbone and Hyp areseen to be involved in binding water molecules through a variety of arrangements. On the average, the C=O groups of Gly residues are bound to one water, while the C=Ogroups of Hyp show two sites for hydrogen bonding to water. The OH of Hyp can bind two water molecules at two distinct sites, but not all positions are fully occupied. Waters bridge two categories of groups in this peptide: water molecules may link two carbonyl groups or they may link one carbonyl group with a hydroxyl group of Hyp. The number of waters involved in bridging two groups appears to vary along the molecule, such that two, three, four, or even five water molecules may form a chain linking the two groups. The water molecules may be linking two groups

on the same chain, e.g., (Gly) C=O··W··O=C(Hyp) (Fig. 2 b, c). Linkages are also seen between groups on two different chains within a molecule, e.g., Chain A Hyp(OH)··W··O=C(Hyp) Chain B (Fig. 2c) [11], [12].

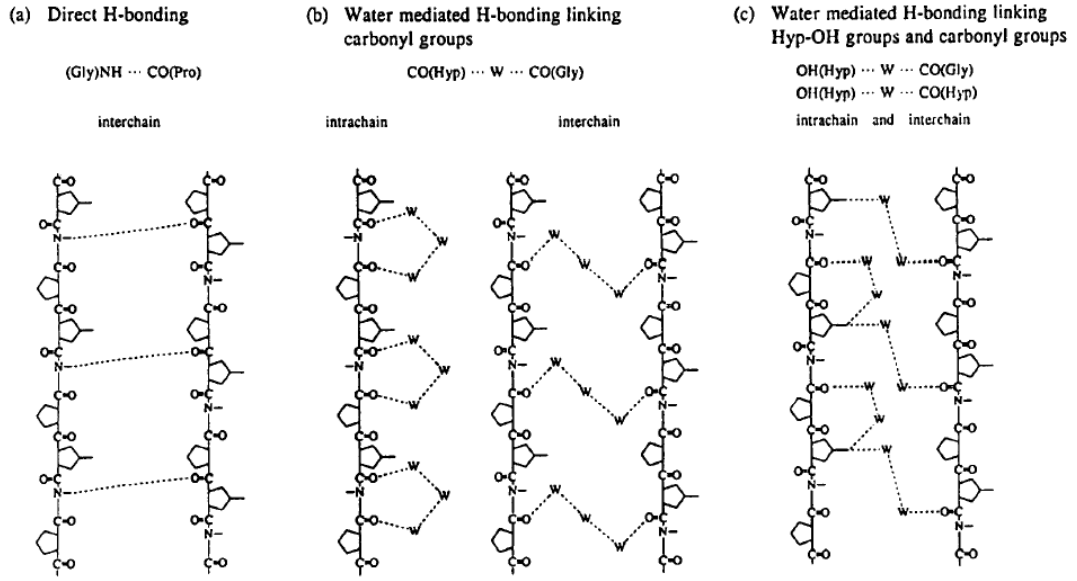

Fig. 2: A schematic drawing illustrating the types of hydrogen bonding patterns found in the triple-helix: (a) direct peptide group hydrogen bonding; (b) water mediated hydrogen bonding linking carbonyl groups; and (c) water mediated hydrogen bonding linking hydroxyproline OH groups and carbonyl groups [11].

In the crystal structure, water bridges are also observed to be the critical element in connecting adjacent triple-helical molecules and maintaining the intermolecular spacing. The distance between adjacent molecules in the crystal is 14 Å, a value very similar to that seen for the lateral packing of collagen molecules in tendon, skin and all other tissues examined by fiber diffraction. It was surprising to find little or no direct contact between neighboring molecules (Fig. 2). Rather, the distance between molecules is maintained by the water molecules which connect adjacent helices. This suggests that the lateral molecular packing of collagen molecules may be determined largely by their hydration shell, which is linked to backbone carbonyls and Hyp [11].

The role of hydroxyproline in the triple helix is to stabilize the polyproline II extended conformation of the individual chains in the triple helix because of the stereochemical restrictions of the imino acid rings. But Hyp was shown to confer a greater stability than Pro in the Y position, and this stabilization was shown to be stereospecific and dependent on being in the Y position. Hydroxyl group of Hyp could not directly hydrogen bond to the carbonyl groups within the same molecule, but is mediated through bridging water molecules. This was confirmed with the crystal structure, which now offers details about the special role of this unusual residue. The hydroxyl group can act as a hydrogen bond acceptor and donor, and water molecules can bind at two different sites. It plays a pivotal role in creating the ordered water shell around the triple-helix. Hyp hydroxyl groups linked by water molecules to a Gly C=O within the same chain, and to the Hyp C=O of the adjacent chain, are sufficient to satisfy all hydrogen bonding potential in the chains (Fig. 2c) [11].

In the $(Gly\text{-}X\text{-}Y)_{338}$ sequence of type I collagen, only about 10 % of the triplets are Gly-Pro-Hyp. The remaining triplets consist of about 20 frequent triplets found more than 1 %

in the sequence and approximately 70 other triplets found one to three times in the sequence. It seems likely that the common Gly-Pro-Hyp, Gly-Pro-Ala and Gly-Ala-Hyp triplets are required for stability of the triple-helix, while triplets containing charged and hydrophobic residues function as sites of recognition involved in biological specificity. Clarification of the molecular basis of recognition and binding of a collagen sequence to another molecule requires an understanding of how variable $(GIy\text{-}X\text{-}Y)_n$ amino acid sequences affect basic properties of the triple-helix, such as the helical parameters, hydration, dynamics and potential interactions [11], [13].

2.1.2 Solubility of collagen

Collagen can be solubilized into an aqueous solution, particularly in acidic aqueous media, and can be engineered to exhibit tailor-made properties [6]. The major impediment to dissolution of collagen type I from tissue is the presence of covalent crosslinks between molecules. Collagen is insoluble in organic solvents. Watersoluble collagen represents only a small fraction of total collagen and the amount depends on the age of the animal and type of tissue extracted. The most commonly used solvents are neutral salt solution (0.15 – 2 M NaCl), dilute acids or pepsin [7].

Neutral salt solutions will extract freshly synthesized and negligibly crosslinked collagen molecules present in the tissue. Modifications in temperature, shaking rate, and volume of extractant to tissue ratio will inevitably alter the composition of the collagen derived. The extracted material is purified by dialysis, precipitation, and centrifugation. Most tissues have little or no salt-extractable collagen[7].

Dilute acidic solvents, e.g. 0.5 M acetic acid, citrate buffer, or hydrochloric acid pH 2 – 3 are more efficient than neutral salt solutions. The intermolecular crosslinks of the aldimine type are dissociated by the dilute acids and the repulsive repelling charges on the triple-helices lead to swelling of fibrillar structures. Dilute acids will not dissociate less labile crosslinks such as keto-imine bonds. Therefore collagen from tissues containing higher percentages of keto-imine bonds, i.e. bone, cartilage, or material from older animals have a lower solubility in dilute acid solvents. In order to acid extract collagen, generally, tissue is ground in the cold, washed with neutral saline to remove soluble proteins and polysaccharides, and the collagen extracted with a low ionic strength, acidic solution. By these methods it is possible to solubilize approximately 2 % of the tissue collagen. These collagen molecules can be reconstituted into large fibrils with similar properties as native fibrils by adjusting the pH or temperature of the solution [7], [14].

The remaining 98 % is referred to as insoluble collagen. Although this collagen material is not absolutely insoluble and can be further disintegrated without major damage to the triple-helical structures. The two most common approaches are the use of strong alkali or enzymes like pepsin [14] to cleave additional crosslinks and suspend or dissolve at first acid-insoluble structures.

Collagen solutions contain varying proportions of monomer and higher molecular weight covalently linked aggregates, depending on the source and method of preparation. Truly monomeric solutions are difficult if not impossible to obtain. Soluble collagen can be stored frozen or lyophilized. In the course of drying, denaturation or non-specific crosslinking can occur and the degree of association upon reconstitution can change [7].

2.1.3 Hydrolysis of collagen

Collagen in solution subjects progressive hydrolytic degradation accompanied by the loss of many physical properties.The speed of this process depends on the temperature, the pH of the system and to a lesser extent on the internal pressure of the solution and the nature of others solvents that may be presented. With higher temperature speed of hydrolysis is growing. At neutral pH degradation occurs slower,with the movement on both sides the speed is increasing [9]. Insoluble native collagen must be pre-treated before it can be converted into a form suitable for extraction, which is normally done by heating in water at temperatures higher than 45 °C. Achemical pre-treatment will break non-covalent bonds so as to disorganize the protein structure. Subsequent heat treatment cleaves the hydrogen and covalent bonds to destabilize the triple-helix, resulting in helix-to-coil transition and conversion into soluble gelatin. The degree of collagen conversion into gelatin is related to the severity of both the pretreatment and the warm-water extraction process, as a function of pH, temperature, and extraction time [8].

2.2 Gelatin

Gelatin is a soluble protein compound obtained by partial hydrolysis of collagen, the main fibrous protein constituent in bones, cartilages and skins. We know two types of gelatin. First one is type-A gelatin (isoelectric point at pH ~8 – 9) and second one is type-B gelatin (isoelectric pointat pH ~ 4 – 5) obtained under acid and alkaline pre-treatment conditions. Industrial applications call for one or the other gelatin type, depending on the degree of collagen crosslinking in the raw material [8], [15].

The molecular structures of gelatin, including its renaturation level, depend on the interactions between water and protein molecules. Consequently, water content has a great influence on the mechanical properties of protein films. An analysis of the literature data on hydration of gelatin makes it possible to subdivide the sorbed water according to its state into four types:

- Water bound by high-energy sorption centres (from 0 to 0.055 g/g (0 – 10 % relative hydratation)). This water sits at charged residues and inside the triple helix and plays a major role in its stabilization through intramolecular hydrogen bonds.
- Structural water (from 0.055 to 0.14 g/g (10 – 40 % relative hydratation)). This is the water directly bound to the protein (both inside and outside helical fragments).
- Polymolecular layer (from 0.14 to 0.37 g/g (40 – 90 % relative hydratation)). In excess of bound water concentration of 0.14 g/g, the monomolecular layer transforms into a polymolecular layer, which covers the triple helix structure.
- Free water (above 0.37 g/g (90 % relative hydratation)). Above 0.37 g/g free non-bound water is observed [16], [18].

2.3 Circular dichroism (CD)

2.3.1 Basic principles of CD

Plane polarized light can be viewed as being made up of two circularly polarized components of equal magnitude, with one rotating counter-clockwise (left-handed circularly polarized, LCP) and the other one rotating clockwise (right-handed circularly polarized, RCP). CD refers to the differential absorption of LCP and RCP lights; this differential absorption occurs on chiral compounds. A CD signal will be observed when a compound is chiral (optically active) for one of the following reasons: (a) it is intrinsically chiral because of its structure, for example, a C atom with 4 different substituents, or the disulphide bond which is chiral because of the dihedral angles of the C–S–S–C chain of atoms, (b) it is covalently linked to a chiral centre in the molecule, or (c) it is placed in an asymmetric environment by virtue of the 3-dimensional structure adopted by the molecule. In a CD instrument (Fig. 3), plane polarized light is split into LCP and RCP lights by passage through a modulator, subjected to an alternating electrical field. The modulator generally is composed of a piezoelectric quartz crystal and a thin plate of isotropic material. The alternating electrical field induces structural changes in the quartz crystal, which cause the plate to transmit circularly polarized light at the extremes of the field. As the transmitted light is switched between LCP and RCP lights, these are detected in turn by the photomultiplier. If one of the lights is absorbed by the sample to a greater extent than the other, the resultant lights would be elliptically polarized, i.e. the resultant would trace out an ellipse (Fig. 4). In practice, the CD instrument does not recombine the lights but detects the two lights separately; it will then display the dichroism at a given wavelength of light expressed as the difference in absorbance (ΔA) of the two light components. A CD spectrum is obtained when the dichroism is measured as a function of wavelength (Fig. 4) [17].

CD instruments (known as spectropolarimeters) measure the difference in absorbance between the L and R circularly polarised components (1).

$$\Delta A = A_L - A_R \qquad (1)$$

But CD is generally expressed in terms of the ellipticity and more often in millidegrees (m° or mdeg). It should be noted that:

$$\theta = tan^{-1}(b/a) \qquad (2)$$

where b and a are the minor and major axes of the resulting ellipse (Fig. 4). There is a simple numerical relationship between ΔA and ellipticity shown in equation (3) [17], [19], [20].

$$\theta = 32.982 \times \Delta A \qquad (3)$$

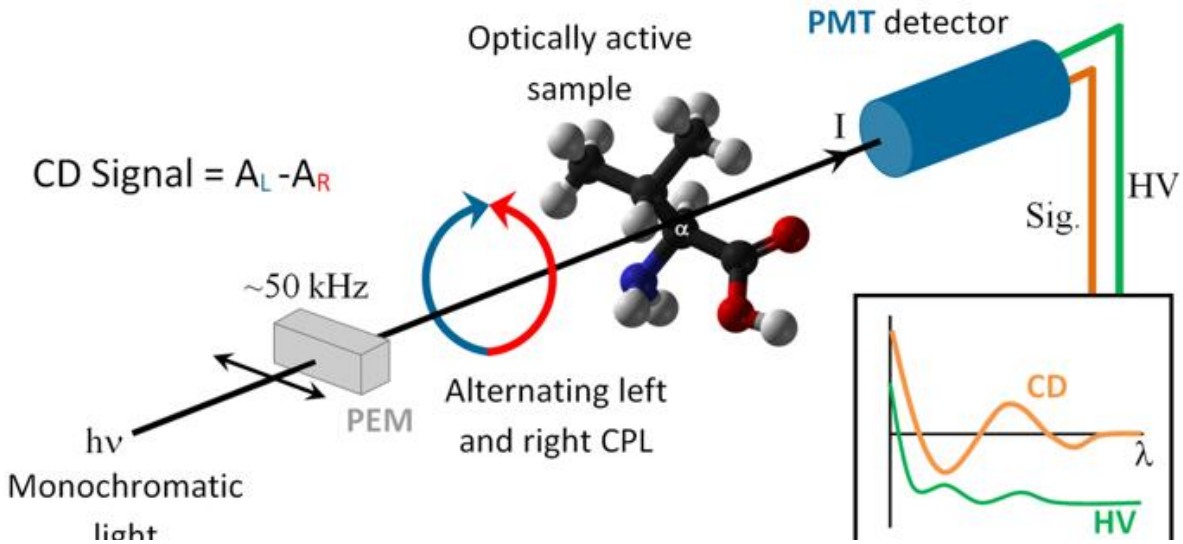

Fig. 3: Scheme of a CD spectrophotometer [21].

There are various methods by which the CD effect can be measured in a spectropolarimeter: (a) modulation, in which the incident radiation is continuously switched between the L and R components, (b) direct subtraction, in which the absorbances of the 2 components are measured separately and subtracted from each other, and (c) ellipsometric, in which the ellipticity of the transmitted radiation is measured [22]. In such a CD instrument (Fig. 4), plane polarised light is split into the L and R components by passage through a modulator subjected to an alternating electric field (50 kHz is the frequency most commonly employed).

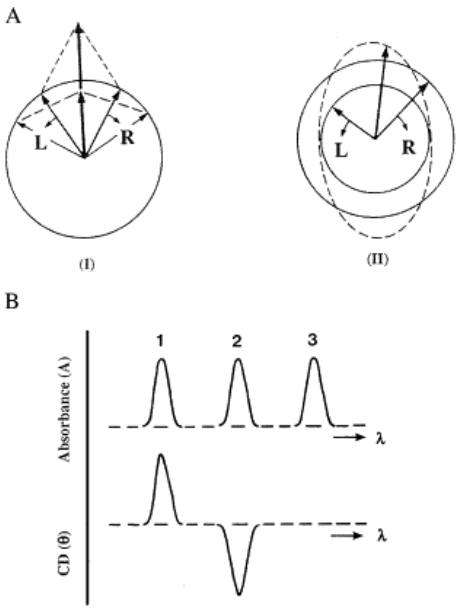

Fig. 4. Origin of the CD effect. (A) The left (L) and right (R) circularly polarised components of plane polarised radiation: (I) the two components have the same amplitude and when combined generate plane polarised radiation; (II) the components are of different magnitude and the resultant (dashed line) is elliptically polarised. (B) The relationship between absorption and CD spectra. Band 1 has a positive CD spectrum with L absorbed more than R; band 2 has a negative CD spectrum with R absorbed more than L; band 3 is due to an achiral chromofore [17].

2.3.2 Measurement of collagen by CD spectroscopy

General signal processing is performed by comparing the signals from different CD spectra in order to figure out signal diference. However, almost all biological studies shows that observed CD signals are very small for proteins, i. e. ellipticities are typically in the range 10 mdeg, corresponding to a difference in absorbance of the order of 3×10^{-4}. It is therefore especially important in CD work to pay attention to the experimental conditions in order to ensure that meaningful data are obtained [17], [19], [20]. CD signals can be measured when absorption of radiation occurs, and thus spectral bands are easily assigned to distinct structural features of a molecule.

The types of information which can be obtained from CD studies of proteins include secondary structure composition from the peptide bond region. Absorption in region 240 nm and below is due principally to the peptide bond; there is a weak but broad $n\rightarrow\pi^*$ transition centred around 220 nm and a more intense $\pi\rightarrow\pi^*$ transition around 190 nm. It is possible to obtain estimates of the a-helical content of peptides and proteins from more limited data by using the values of the CD signals at 208 nm and 222 nm [17], [19]. However, it must be emphasised that these estimates are to be treated with caution and, if at all possible, CD data should be gathered over a more extended range of wavelengths in the far UV. It must be emphasised that for reliable analysis of secondary structure, it is necessary to ensure that the concentration of the protein solution is accurately known and that the CD instrument is properly calibrated and operand [17].

Measurement of collagen by CD in solid state

Leah C. Abraham with team studied collagen prepared on silica Windows [4]. They firstly dissolved collagen at 2 – 8 °C in sterile filtered 0.1% glacial acetic acid (GAA) at 5 – 10 mg/ml over at least 3 days for complete dissolution. Once dissolved, the solution of collagen is diluted to working concentrations just before use to generate the nondenatured (native) biomaterial surfaces. Denaturation is accomplished during 60 min treatment in a 50 °C water bath. CD data were collected using a Jasco J-710 Spectropolarimeter at 25 °C from 190 to 260 nm with 0.05 nm step resolution, 10 nm/min collection, an accumulation rate of 4, response of 16 s, band width at 1.0 nm, and sensitivity of 50 mdeg. Data were considered valid for the range of the instrument when the ‘‘HT’’ (Jasco labeling of voltage) photomultiplier voltage was below 650 V. CD for collagen solutions was collected at a concentration of 0.125 mg/ml. For collagen films, drops of ~100 µl of 0.5 µg/µlcollagen were dried on quartz Suprasil 0.01 mm flat cuvette plates from Hellma for analysis. CD was used to examine helical content as a function of heat denaturation (temperature melts), as a reflection of structure and chemistry. For both native and denatured (1 h, 50 °C heat treated) collagen, the helical content of the collagen solutions and the films was confirmed by CD (Fig. 5). The CD curve for the nondenatured collagen shows the expected profile for a helical collagen molecule including maxima at 225 nm and minima at 201 nm. Both of the denatured collagen samples show a significant decrease in the positive peak from 225 nm as well as a significant reduction in the negative peak from 201 nm. These data confirm the helical content of the nondenatureted collagen and also indicate a significant reduction of helical content for denatured collagen that had been heattreated. There was no significant difference in helicity as a function of the concentration at which the collagen was heat-treated.

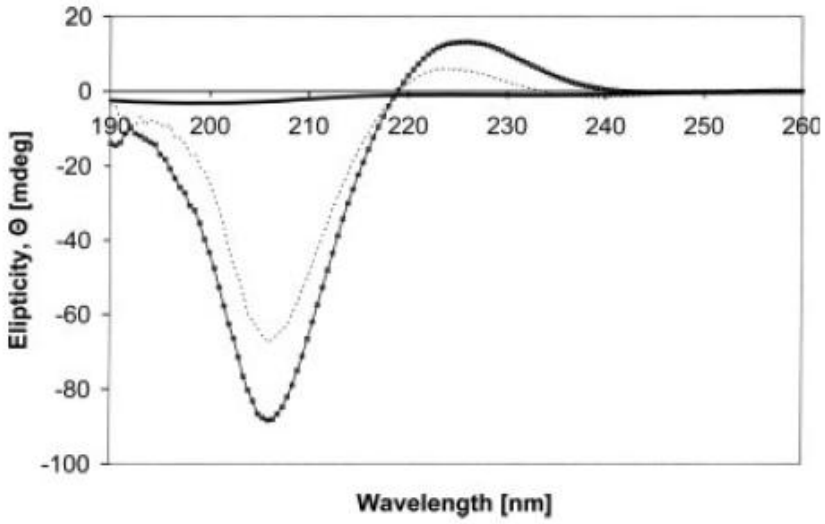

Fig. 5: CD on collagen solutions. Shown are the elipticity data for collagen films, where 100 µl of 0.5 mg/ml of collagen was dried directly on quartz Suprasil 0.01 mm flat cuvette plates: (- -) Denatured, (—) Gelatin, (■) Nondenatured [4].

JingWang with team measured CD spectra to assess the secondary structure [14]. CD spectra were determined using a MOS-450 CD spectrometer. Acid soluble collagen (ASC) and pepsin soluble collagen (PSC) were diluted to 0.3 mg/ml with 0.05 M acetic acid. CD spectra were obtained using a 0.1 cm path-length quartz cell. Three scans were averaged at 190 – 250 nm. The CD spectrum of protein provides information on the protein secondary structure [17], [19]. Fig. 6 represents a characteristic CD spectrum of ASC at 15 °C with a positive peak at 217 nm and a negative peak at 197 nm. The CD spectrum of PSC had a similar profile to that of ASC. These unique spectra were characteristic of a triple helical structure [12].

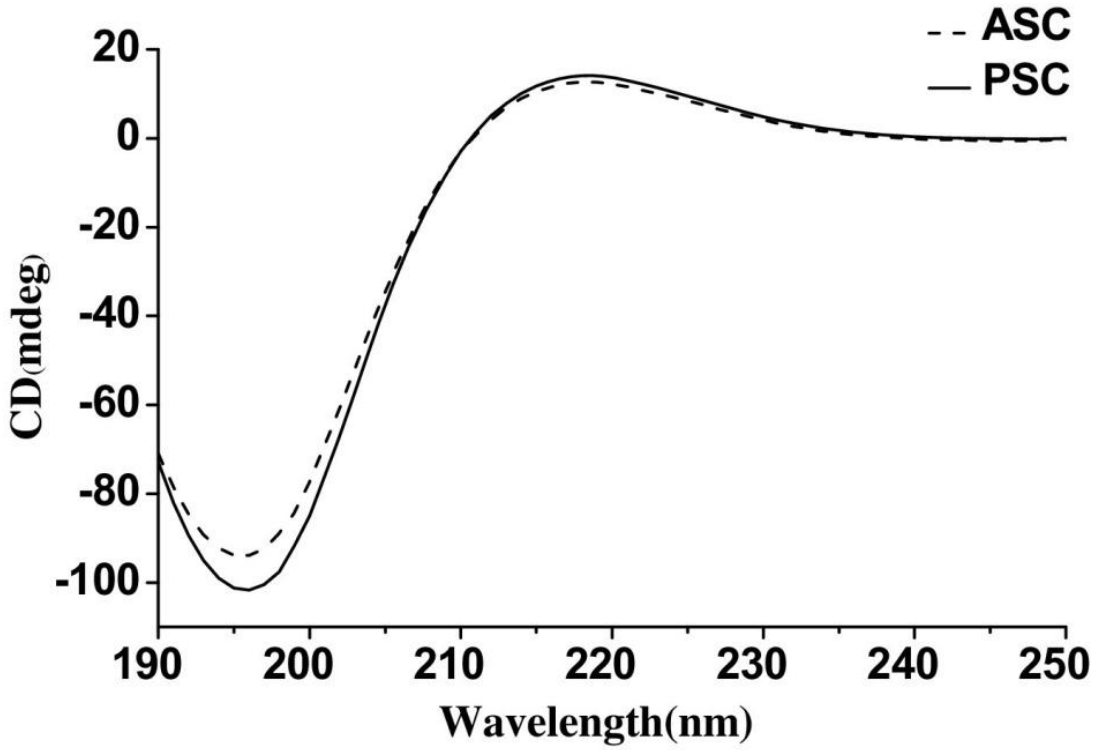

Fig. 6: CD spectra of ASC and PSC from the skin of the loach at 15 °C [14].

Ali Muhammed Moula Ali with team extracted ASC a PSC from golden carp scales [24], [25]. All the procedures for pretreatment, washing and extraction were carried out at 4 °C to avoid denaturation of collagen. Extraction of ASC was performed by method [26] with a slightly modification. The undissolved residue gained after ASC extraction was used to extract PSC. The residue was extracted with acetic acid (0.5 M) containing 1% pepsin (w/w) at a residue/solution ratio of 1/10 (w/v). The extraction was performed with the aid of continuous stirring for 24 h at 4 °C. Subsequently, the extracted collagen was filtered and precipitated in the similar fashion as described for ASC [24], [25].

Next one was prepared acid soluble collagen extracted by ultrasound assisted method (UASC). Skin (100 g) was soaked in 0.5 M acetic acid with a skin/acid solution ratio of 1/15 (w/v). The skin was allowed to swell partially by holding the mixture for 30 min at 4 °C. The mixture was subjected to ultrasonication. The reaction was carried out at a power of 750 W, working at a single frequency of 20 kHz. The temperature of the sample was maintained at 4 °C using an ice bath. To avoid overheating, the ultrasound was operated in a pulse mode at 5 s acting and 5 s resting time. The treatment was conducted at different levels of amplitude (20, 50 and 80 %) for various times (10, 20, 30 min). After the treatment, further extraction was carried out for 48 h by continuous stirring. Collagen was precipitated, dialysed and lyofilized as mentioned above [25].

For PSC prepared using ultrasound assisted process (UPSC), skin (100 g) was suspended in 0.5 M acetic acid solution with a skin/acid solution ratio of 1/15 (w/v). To mixture was added 1% pepsin. The skin was allowed to partially swell as stated above and subjected to ultrasonication at 80 % amplitude for 30 min using the pulse mode as described previously. Further extraction was done and PSC was collected, dialysed and lyofilized [25].

ASC and PSC (2.0×10^{-4} g/ml) were prepared by dissolving in 0.5 M acetic acid. The spectra were obtained via scanning in the wavelength range of 190 to 240 nm using JASCO J-801 spectrometer with a bandwidth rate of 1 nm. The measurements were recorded at 25 °C by maintaining nitrogen gas as an atmosphere. Acetic acid (0.5 M) was used as blank, which was then subtracted from the average of samples spectra. The obtained results were expressed as the molar residual ellipticity [25].

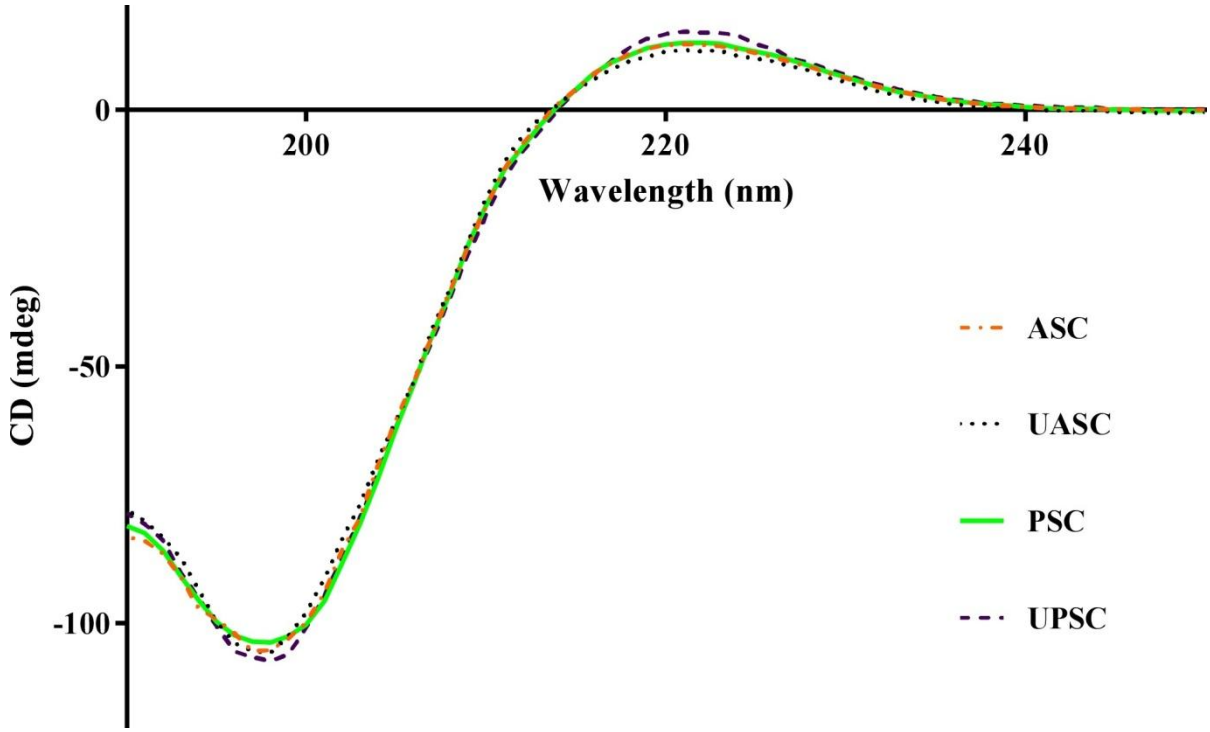

Fig. 7: CD spectra of ASC, PSC, UASC and UPSC from the scales of golden carp at 25 °C [25].

The triple helical conformation of ASC, UASC, PSC and UPSC was confirmed by CD spectra in Fig. 7. A distinctive positive peak at 221 nm and a negative peak at 198 nm are ideal for collagen [27]. The rotatory maxima of the positive peak of ASC and UASC were at 220 and 219.9 nm. The similar molar ellipticity between ASC and UASC indicated no difference in the secondary structure. Thus ultrasound treatment had no impact on the secondary structure of resulting collagen. For PSC and UPSC, positive peaks were at 220,8 and 221 nm. The molar ellipticity of UPSC was higher than that of PSC, ASC and UASC. This result indicated that UPSC had more compact on triple helical structure. It has been reported that PSC has more ordered secondary structure than that of ASC, as the pepsin removes non-helical telopeptide region from the molecules [28]. In the present study, it was observed that cavitation induced by ultrasound facilitated pepsin to cleave telopeptide region more effectively. As a result, more amounts of collagen were released [29], [30]. All the collagens also showed a negative peak at 198 nm. The CD spectra of denatured collagen loses the positive peak and shifts the negative peak to the lower wavelength [27].

Qiufang Liang with team characterized collagen from the cartilage of Amur sturgeon [28]. The isolation procedure of salt-, acid- and pepsin-solubilized collagen (SSC, ASC and PSC) from Amur sturgeon cartilage was done following these steps. Cartilage was pretreated by homogenizing for 5 min and soaking in 0.1 M NaOH, 0,5 M EDTA (pH 7.4) and hexane at 1/20 (w/v) for 12 h for 2 times. Salt-solubilized collagen (SSC) was then extracted using 0.45 M NaCl at the ratio of 1/100 (w/v) for 24 h with continuous stirring. After centrifuging at 20 000 × g for 60 min, the pellet was re-extracted until no collagen dissolved. All the supernatants were combined and salted-out by the addition of NaCl to 2.0 M in acidic conditions. The precipitate was obtained by centrifugation at 2 500 × g for 20 min, and then redissolved, dialyzed and lyophilized. The residue after salt extraction was suspended in 0.5 M acetic acid for the extraction of acid-solubilized collagen (ASC). The insoluble matter in acetic acid was then used to extract pepsin-solubilized collagen (PSC) using 0.1% (w/v) pepsin in 0.01 M HCl. All the other preparation procedures of ASC and PSC were performed as described for SSC. All operations were carried out at 4 °C. The yields of SSC, ASC, PSC were 2.18 %, 27.04 % and 55.92 %, estimated by hydroxyproline content in prepared collagen and pretreated cartilage [28].

The molecular conformation was assessed by CD spectra using a spectropolarimeter (Jasco, J-815). The collagen was dissolved in 0.01 M HCl to a concentration of 0.02 mg·ml^{-1}, and then placed into a quartz cell with a path length of 10 mm. The spectrum from 190 nm to 250 nm was recorded with an interval of 0.5 nm and scan speed of 50 nm·min^{-1} under nitrogen atmosphere at 20 °C [28]. As seen in Fig. 8, the CD spectra of collagen showed a rotatory maximum at 221 nm, a minimum at 198 nm and a consistent crossover point at about 213 nm, which is a typical characteristic of triple helical conformation of collagen [28], [31], [32].

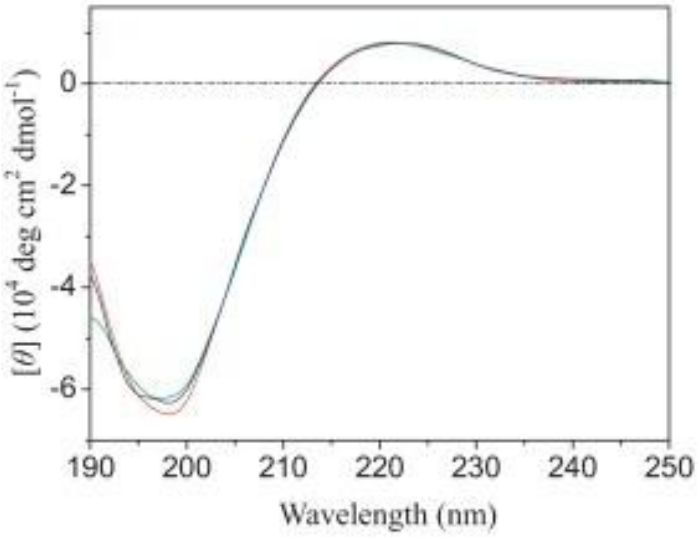

Fig. 8: CD spectra of ASC (green), PSC (blue) and SSC (red) from the cartilage of Amur sturgeon [28].

2.4 Infrared spectroscopy (IR)

2.4.1 Basic principles of IR

Infrared spectroscopy is a technique based on the vibrations of the atoms of a molecule. An infrared spectrum is commonly obtained by passing infrared radiation through a sample and determining what fraction of the incident radiation is absorbed at a particular energy. The energy at which any peak in an absorption spectrum appears corresponds to the frequency of a vibration of a part of a sample molecule. One of the great advantages of IR is that any sample in any state may be studied. Liquids, solutions, pastes, powders, films, fibres, gases and surfaces can all be examined with a judicious choice of sampling technique. For a molecule to show infrared absorptions it must possess a specific feature, i.e. an electric dipole moment of the molecule must change during the vibration. This is the selection rule for infrared spectroscopy [23], [33].

Modern infrared spectrometers are usually Fourier transform infrared spectrometers (FTIR). Their name originates from the fact that the detector signal of these spectrometers is related by a Fourier transformation to the measured spectrum. The heart of an FTIR spectrometer is an interferometer, like the Michelson interferometer shown in Fig. 9. It has a fixed and a movable mirror. The latter generates a variable optical path difference between two beams which gives a detector signal that contains the spectral information. Light emitted from the light source is split by a beam splitter: about half of it is reflected towards the fixed mirror and from there reflected back towards the beamsplitter where about 50 % passes to reach the detector (black arrows in Fig. 9). The other half of the initial light intensity passes the beam splitter on its first encounter, is reflected by the movable mirror back to the beamsplitter where 50 % of it is reflected towards the detector (grey arrows in Fig. 9). When the two beams recombine they interfere and there will be constructive or destructive interference depending on the optical path difference d. The instrument measures the light intensity relative to the position of the movable mirror and this is called an interferogram. It turns out that the interferogram is the Fourier transform of the spectrum. A second Fourier transform performed by a computer converts the measured data back into a spectrum. In total, a Fourier transform spectrometer performs two Fourier transformations: one by the interferometer, one by the computer. That the interferometer produces the Fourier transform of the spectrum is best seen when a monochromatic source is considered. Its spectrum $S(\lambda)$ is described by a delta function located at λ_0. Depending on the position of the movable mirror one obtains constructive or destructive interference at the detector and the detector signal $I(d)$ varies as a cosine function with the mirror position which determines the optical path difference d. This cosine function and the delta function describing the monochromatic spectrum are related by a Fourier transformation. Thus, a second Fourier transformation performed by the computer generates the spectrum $S(\lambda)$ [23], [33].

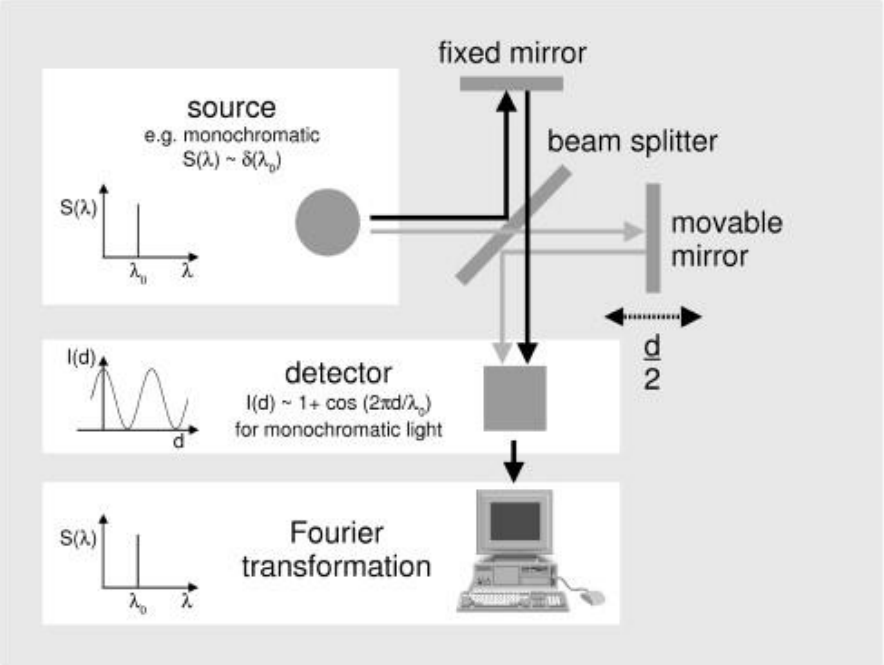

Fig. 9: Scheme of a Fourier transform infrared spectrometer [33].

2.4.2 Attenuated total reflectance (ATR) spectroscopy

Attenuated total reflectance (ATR) spectroscopy utilizes the phenomenon of total internal reflection (Fig. 10). A beam of radiation entering a crystal will undergo total internal reflection when the angle of incidence at the interface between the sample and crystal is greater than the critical angle, where the latter is a function of the refractive indices of the two surfaces. The beam penetrates a fraction of a wavelength beyond the reflecting surface and when a material that selectively absorbs radiation is in close contact with the reflecting surface, the beam loses energy at the wavelength where the material absorbs. The resultant attenuated radiation is measured and plotted as a function of wavelength by the spectrometer and gives rise to the absorption spectral characteristics of the sample. The depth of penetration in ATR spectroscopy is a function of the wavelength, λ, the refractive index of the crystal, n_2, and the angle of incident radiation, θ. The crystals used in ATR cells are made from materials that have low solubility in water and are of a very high refractive index. Such materials include zinc selenide (ZnSe), germanium (Ge) and thallium–iodide (KRS-5). Different designs of ATR cells allow both liquid and solid samples to be examined [23], [33], [34].

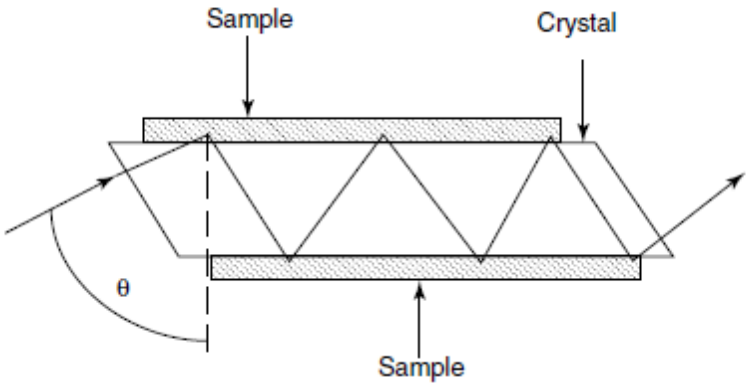

Fig. 10: Schematic of a typical attenuated total reflectance cell [23].

2.4.3 Measurement of collagen by ATR spectroscopy

The ATR technique is illustrated in Fig. 11. Compared to transmission experiments, it avoids the handling problems which are caused by the required short pathlength. In an ATR experiment a sample is placed on a crystal with an index of refraction that is larger than that of the sample and typically larger than 2. Infrared light is coupled into the crystal and directed towards the sample interface at such an angle of incidence that it is totally reflected at the interface between sample and crystal. After one or several reflections the measuring light leaves the crystal and is focused on the detector. Upon reflection at the interface between sample and crystal, light penetrates into the sample. This so-called evanescent wave has the same frequency as the incoming light but the amplitude of the electric field decays exponentially with the distance from the interface. The evanescent wave may be absorbed by the sample and thus the light reaching the detector carries the information about the infrared spectrum of the sample. The penetration depth is on the order of the wavelength, which means that the optical thickness of the sample is small enough for measurements of aqueous solutions. The penetration depth depends also on the angle of incidence and the ratio of the indices of refraction of crystal and sample [23], [33], [35], [36].

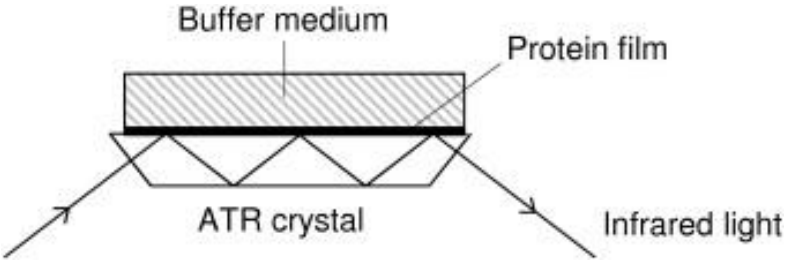

Fig. 11: A typical ATR setup for meassuring of protein films [33].

For protein samples, usually a protein film is prepared on the crystal surface [33], [37], often simply by drying, and a buffer is placed on top of the film. The thickness of the buffer layer does not influence the measured spectrum. The advantage of the method is that often the buffer can be exchanged without disturbing the film [33].

2.4.4 Absorbance of collagen (amide I, amide II)

The amide I vibration, absorbing near 1650 cm^{-1}, arises mainly from the C=O stretching vibration with minor contributions from the out-of-phase CN stretching vibration, the CCN deformation and the NH in-plane bend. The latter is responsible for the sensitivity of the amide I band to N-deuteration of the backbone. In proteins, the extent to which the several internal coordinates contribute to the amide I normal mode depends on the backbone structure [14], [16], [33], [38], [39]. The amide I vibration is hardly affected by the nature of the side chain. It depends however on the secondary structure of the backbone and is therefore the amide vibration that is most commonly used for secondary structure analysis.

Experimental studies have indicated a number of rules of thumb that describe how the amide I absorption depends on backbone structure. α-helices give rise to a main absorption band close to 1 655 cm^{-1} and a shoulder at lower wavenumbers [40], [41]. The band position of the main band shifts down with increasing helix length [40], when the helix is bent in coiled coils [42], [43] and when the helix is solvent exposed (absorption

maximum at 1 640 – 1 650 cm^{-1} in ^1H_2O, at 1 629 – 1 640 cm^{-1} in ^2H_2O) [44], [45], [46], [47]. Short α-helices with less than 6 residues do not always give rise to the typical α-helix absorption but can produce several bands throughout the amide I region [40], [41]. Antiparallel β-sheets exhibit a strong band near 1 630 cm^{-1} and a weaker band near 1 685 cm^{-1}. The position of these bands is hardly affected by the number of amide groups in the strands of the sheet, but depends on the number of strands. Sheets with a larger number of strands have a lower spectral position of the main band. Also the main band of parallel β-sheets shifts to lower wavenumbers with increasing number of strands [40]. Twisting of an antiparallel β-sheet causes its main band to shift to higher wavenumbers and reduces the splitting between high and low wavenumber band. The effect of twisting is less for parallel β-sheets. Parallel β-sheets [40], [48] have their main absorption at higher wavenumber than corresponding antiparallel β-sheets [40], [48]. The result is that a particular secondary structure absorbs predominantly in a specific range of the amide I region, as specified in Tab. 2 [49].

Tab. 2: Assignment of amide I band positions to secondary structure [49].

Secondary structure	**Band position in ^1H_2O/cm^{-1}**		**Band position in ^2H_2O/cm^{-1}**	
	Average	**Extremes**	**Average**	**Extremes**
α-helix	1654	1648 – 1657	1652	1642 – 1660
β-sheet	1633, 1684	1623 – 1641, 1674 – 1695	1630, 1679	1615 – 1638, 1672 – 1694
Turns	1672	1662 – 1686	1671	1653 – 1691
Disordered	1654	1642 – 1657	1645	1639 – 1654

The amide I band of polypeptides and proteins has long been known to be sensitive to secondary structure and this has caused considerable interest into how structure relates to spectrum. However, explaining the large splitting of the amide I band of β-sheet structures has presented a challenge for theoreticians. The fundamental mechanism that renders the amide I vibration sensitive to secondary structure is transition dipole coupling (TDC) [33], [50]. It is a resonance interaction between the oscillating dipoles of neighbouring amide groups and the coupling depends upon their relative orientation and their distance. Coupling is strongest when the coupled oscillators vibrate with the same frequency. TDC mechanism explains splitting in a main band near 1 630 cm^{-1} and a side band near 1 690 cm^{-1}. Other effects like through-bond coupling and hydrogen bonding also modify the amide I frequency of polypeptides to different degree [33], [51].

The amide II mode is the out-of-phase combination of the NH in plane bend and the CN stretching vibration with smaller contributions from the CO in plane bend and the CC and NC stretching vibrations. Like for the amide I vibration, the amide II vibration of proteins is hardly affected by side chain vibrations but the correlation between protein secondary structure and frequency is less straight forward than for the amide I vibration. Nevertheless it provides valuable structural information and secondary structure prediction can be done with the amide II band alone[33], [52].

Jing Wang with team extracted ASC and PSC from loach skin [14]. These extracted collagens were measured by FTIR. The FTIR spectra of ASC and PSC are presented in Fig. 12. The main characteristic absorption peaks contained amide A, amide B, amide I, amide II, and amide III. Similar findings were reported in other fish species [53], [54], [55]. The amide A bands of ASC and PSC from loach skin were observed at 3 323 and 3 322 cm^{-1}, and involved N–H stretching vibration. N–H stretching vibration ranges from 3 400 to 3 440 cm^{-1} when the amide group of a peptide is associated with a hydrogen bond [56]. This result revealed that the amide groups of loach skin collagen formed hydrogen bonds with carbonyl groups present in the peptide chain. The amide B bands of ASC and PSC were observed at 2 928 and 2 927 cm^{-1}, which are associated with the asymmetrical stretching of CH_2 [57]. The amide I band frequencies from 1 600 to 1 700 cm^{-1} are mainly associated with carbonyl group stretching vibrations and are characteristic of a secondary coil structure [16], [58]. The amide I bands of ASC and PSC were observed at 1 658 and 1 657 cm^{-1}. This observation confirmed that the hydrogen bonds between the amide group and the carbonyl group were responsible for the triple helical structure [59]. Additionally, the results suggested that PSC had more hydrogen bonds than ASC, because of the greater non-helical portion of the telopeptides in ASC [60]. The amide II bands of ASC and PSC were observed at 1 548 and 1 546 cm^{-1}, while the amide III bands of ASC and PSC were located at 1 238 and 1 236 cm^{-1}. The amide II bands corresponded to N–H bending vibrations, and the amide III bands represented C–H stretching [49]. The amide III band revealed the presence of a helical structure [61]. The ratio of absorbance between amide III and the 1 400 – 1 454 cm^{-1} wavelength was 1.0, which revealed that the triple helical structure of collagen was intact. The IR values for ASC and PSC from loach skin (1.10 and 0.99) confirmed the presence of triple helical structures [14], [62].

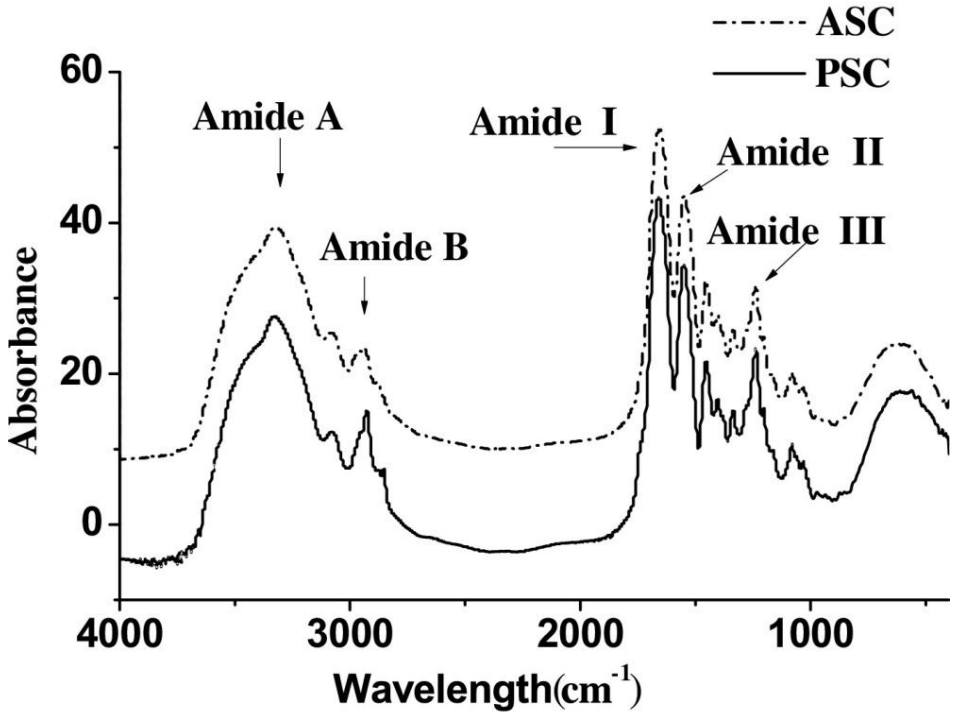

Fig. 12: FTIR spectra of ASC and PSC from the skin of loach [14].

Rui Duan with team try to separete collagen from skin of carp [63]. The skins were mixed with 0.1 M NaOH at a sample/alkali solution ratio of 1/8 (w/v) to remove non-collagenous proteins. The mixture was stirred for 6 h. The alkali solution was changed every 3 h. Then the samples were washed with cold distilled water, until neutral pH of washing water was obtained. Deproteinised skins were soaked in 1.0% detergent at sample/detergent solution ratio of 1/10 (w/v) overnight to extract fat, and then the samples were washed with cold distilled water repeatedly. The treated skins were cut into small pieces by scissor and extracted with 0.5 M acetic acid for 3 days with stirring. The extract was centrifuged at 20 000 g for 1 h. The supernatant were salted-out by adding NaCl to a final concentration of 2.5 M in the presence of 0.05 M tris (hydroxymethyl) aminomethane, pH 7.0. The resultant precipitate was collected by centrifuging at 20 000 g for 30 min. The pellet was dissolved in 0.5 M acetic acid, dialysed against 0.1 M acetic acid and distilled water, and then lyophilised (ASC from skin). Then they analize collagen by FTIR. The FTIR spectra of ASC from carp skin was shown in Fig. 13. Collagens from carp skin had a shifted N-H stretching vibration (3 324.33 cm^{-1}) in infrared spectrum, which meant existence of hydrogen bonds in collagen. The amide I bands position of collagen was 1 649.50 cm^{-1}, fitting in range of 1 625 – 1 690 cm^{-1} for general amide I bands position. The amide II bands position was detected in 1 540 cm^{-1}. Compared to the normal absorption range of the amide II bands position (1 550 – 1 600 cm^{-1}), the position is shifted to lower frequency, which also showed the existence of hydrogen bonds in each collagen [63], [64].

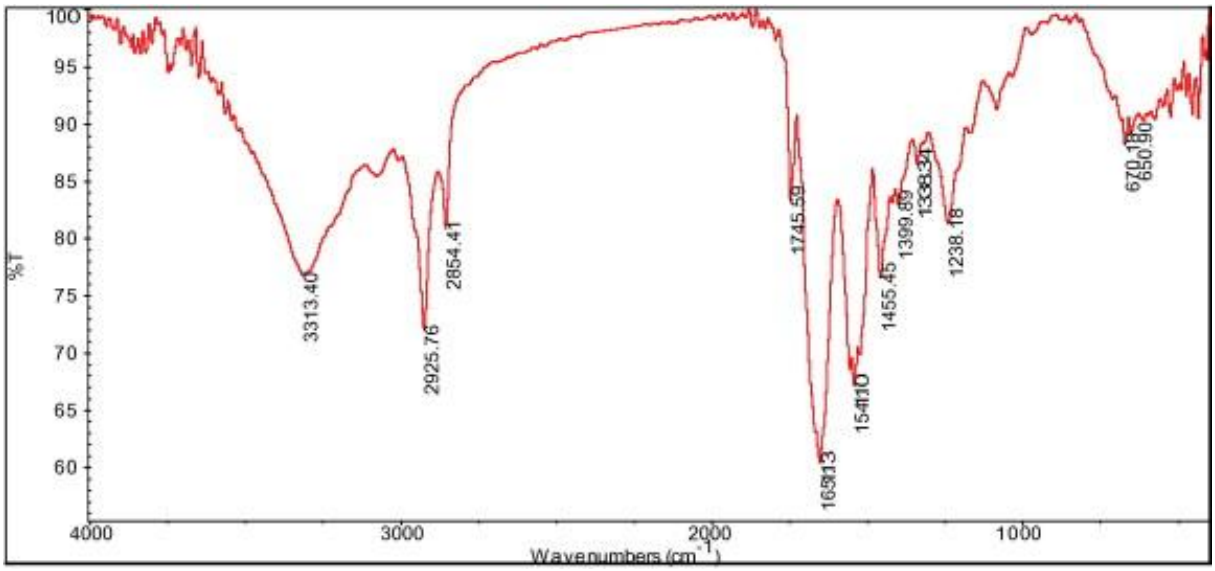

Fig. 13: FTIR spectrum of carp skin ASC [63].

Junjie Zhang with team separated collagen from frog skin [65]. All preparation procedures for ASC and PSC were performed at 4 °C. ASC was isolated and purified following the method described by Rui Duan [63], but also pepsin proteolysis was performed. It suggests that the telopeptide region of the collagen molecule is highly cross-linked [65], [66]. The extractability of PSC significantly improved with the addition of pepsin. Pepsin can cleave the cross-linked regions at the telopeptide can be cleaved without damaging the integrity of the triple helix [65], [67].

The FTIR spectra of frog skin ASC and PSC are shown in Fig. 14. Despite their different absorption intensities, ASC and PSC from frog skin showed similar spectral positions. The intensity of the infrared absorption was related to the transition probability and the size of the dipole moment change in the molecules. High absorption intensity meant high transition probability and dipole moment change. The electronic transitions of the X–H groups (X = C, N, O) from frog skin ASC were simpler and possessed higher dipole moment changes than those of the same groups from frog skin PSC [65].

The amide I band positions of ASC and PSC were detected at approximately 1 632 and 1 630 cm^{-1}, fitting in the range of 1 625 – 1 690 cm^{-1} for general amide I band position. The amide II band positions of ASC and PSC were detected at 1 548 and 1 544 cm^{-1}. Compared with the normal absorption range of the amide II band position (1 550 – 1 600 cm^{-1}), the position shifted to a low frequency, which also showed hydrogen bonds existed in frog skin ASC and PSC. The absorption between the 1 236 and 1 452 cm^{-1} bands (amide III) demonstrates the presence of a helical structure and suggests the helical arrangement of frog skin collagens. The FTIR indicated that the collagens retained their helical structures [65].

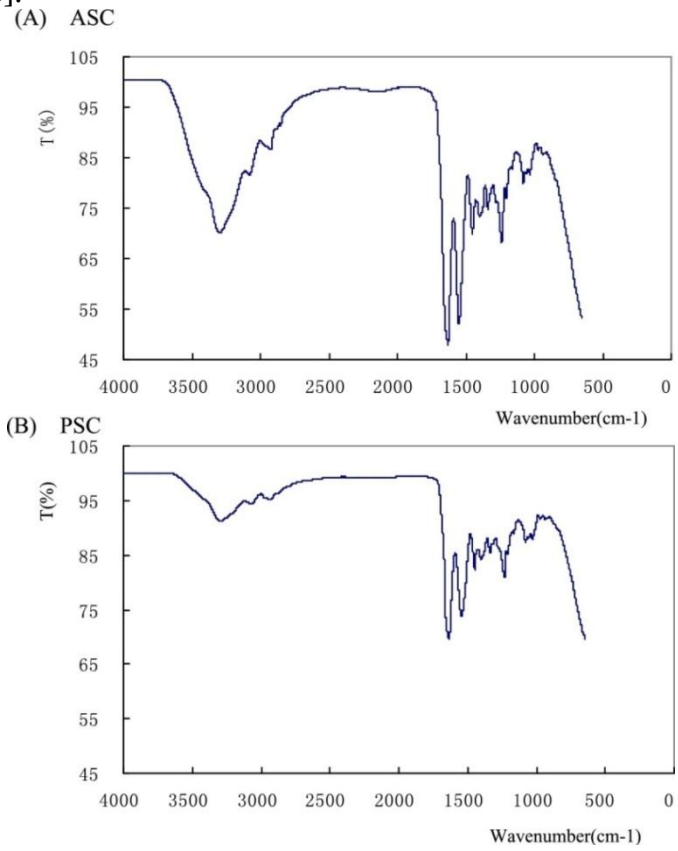

Fig. 14: FTIR spectrum of frog ASC (A) and PSC (B) [65].

Leilei Sun with team extracted ASC and PSC from pacific cod skins [68]. ASC was prepared by following procedures on ice or at 4 °C [69]. The extraction procedures of PSC were similar to ASC. The fish skins after alkali treatment were extracted with 1/60 (v/w) of 0.5 M acetic acid in the presence of 0.5% (w/w) pepsin. The crude extract was depurated via salting-out. Then the resulting precipitate after centrifugation was re-dissolved in 0.5 M acetic acid and dialyzed against 0.02 M Na_2HPO_4 for 48 h to inactivate pepsin followed by 0.1 M acetic acid for 24 h and deionized water for 48 h [68].

1 mg of ASC and PSC samples were mixed with approximately 100 mg dried pottasium bromide (KBr, spectrum pure). Then they were ground and pressed into relatively transparent sheets under dry conditions. The FTIR spectra were recorded from 4 000 to 500 cm^{-1} at a data acquisition rate of 2 $cm^{-1}$with 64 scans [68].

The characteristic absorption peaks of FTIR spectra were shown in Fig. 15. From the spectra, ASC was almost identical to PSC, which was also in agreement with the findings reported by Zhang [70]. The range of a free N–H stretching vibration was 3 400 – 3 440 cm^{-1}, while it could shift near to 3 300 cm^{-1} thanks to the existence of hydrogen bonds [56]. The amide A bands were 3 298.58 cm^{-1} for ASC and 3 308.19 cm^{-1} for PSC, indicating the existence of hydrogen bonds. Both of amide B bands were detected at 2 933.45 cm^{-1}, which was related to CH_2 asymmetrical stretching [57]. The amide I, II, III bands were associated with the carbonyl group stretching vibration coupled with a carboxyl group, N–H bending vibration coupled with a C–N stretching vibration, the combination of C–N stretching, N–H deformation from amide linkages [71]. The corresponding wavelengths were measured at 1 655.52 cm^{-1}, 1 540.21 cm^{-1}, 1 232.74 cm^{-1} for ASC and 1 655.52 cm^{-1}, 1 537.01 cm^{-1}, 1 239.15 cm^{-1} for PSC. Moreover, the absorption ratio of amino III band and CH_2 bending band at 1 450.53 cm^{-1} was close to 1.0, which proved the native and intact triple-helical structure of collagen [57], [72].

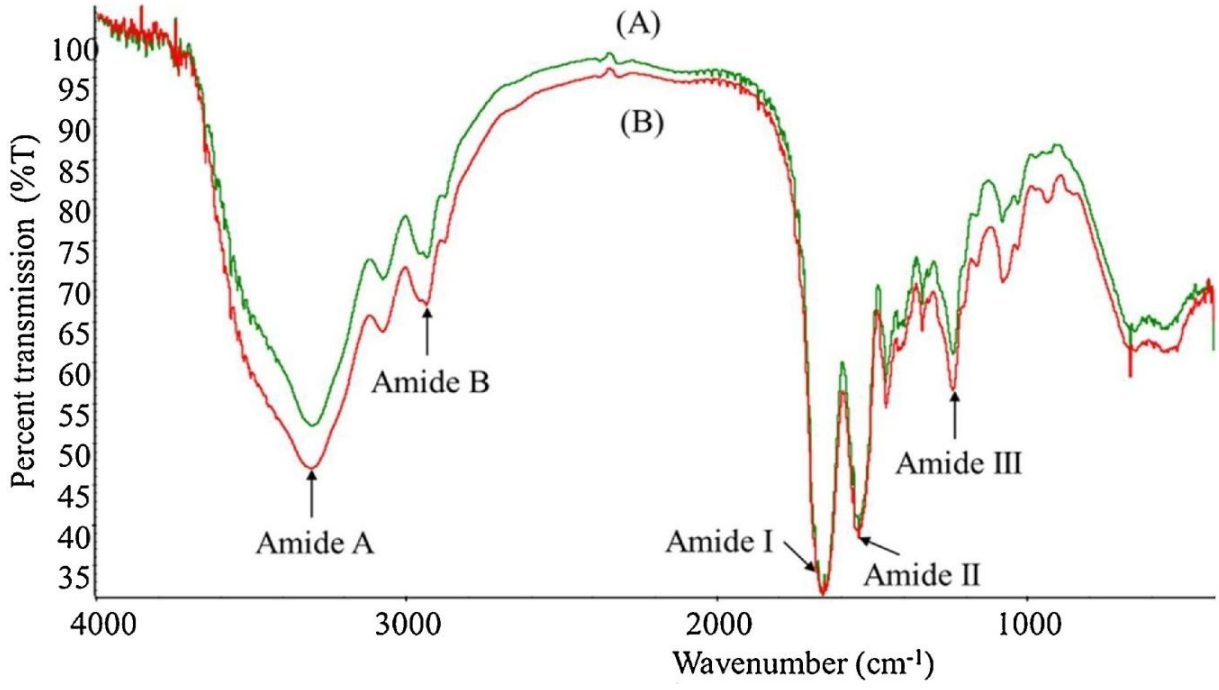

Fig. 15: FTIR spectrum of ASC (A) and PSC (B) from Pacific cod skins [68].

Muyonga with team prepared ASC from skins of young Nile perch [73]. The gelatins used in this study were derived from Nile perch skins and bones by the acid process. FTIR spectra were obtained from discs containing 2 mg sample in approximately 100 mg potassium bromide (KBr). All spectra were obtained using a infrared spectrophotometer from 4 000 to 500 cm^{-1}at data acquisition rate of 2 cm^{-1} per point. Triplicate samples of collagen and gelatins were analysed and spectra for the triplicate runs averaged. Fourier self deconvolution was conducted on the average spectra for the amide I band, using a resolution enhancement factor of 1.8 and full height band width of 13 cm^{-1}. The self deconvolution provided information on the number and location of components. Curve fitting was then performed using peakfit software [73].

The amide I band, between 1 600 and 1 700 cm^{-1}, is the most useful for infrared spectroscopic analysis of the secondary structure of proteins [58]. Deconvolution of the amide I band showed the band to consist of four components. The component peaks and their location are shown in Fig. 16 [73]. The variation in frequencies for particular band components in this investigation was not very different from that reported by [74]. They reported a variation of approximately 15 cm^{-1} for frequencies, attributable to β-structures of various components. Quantitative band-fitting analysis of amide I areas, as applied in this investigation proved useful in studying the nature and the extent of protein conformational changes [58].

Denaturation of collagen lead to reduction in the intensity of amide A, I, II and III peaks [73], [75], narrowing of amide I band [76], increase in amide I component found around 1 630 cm^{-1} and reduction in the intensity of amide I component, found around 1 660 cm^{-1} [77], [78], [79].

Gelatin melting was studied in [76]. They found association with reduction in the 1 678 cm^{-1} peak and 1 660/1 690 cm^{-1} peak intensity ratio and increase in amide I components occurring around 1 613, 1 629 and 1 645 cm^{-1}. These authors assigned the bands occurring at 1 645 – 1 657 $cm^{-1}$to random coils and the 1 660 cm^{-1}band to triple helix, with contribution from α-helix and β-turns. The amide I component, at 1 690 cm^{-1}, has been attributed to helices of aggregated collagen-like peptides [56], [73], [76].

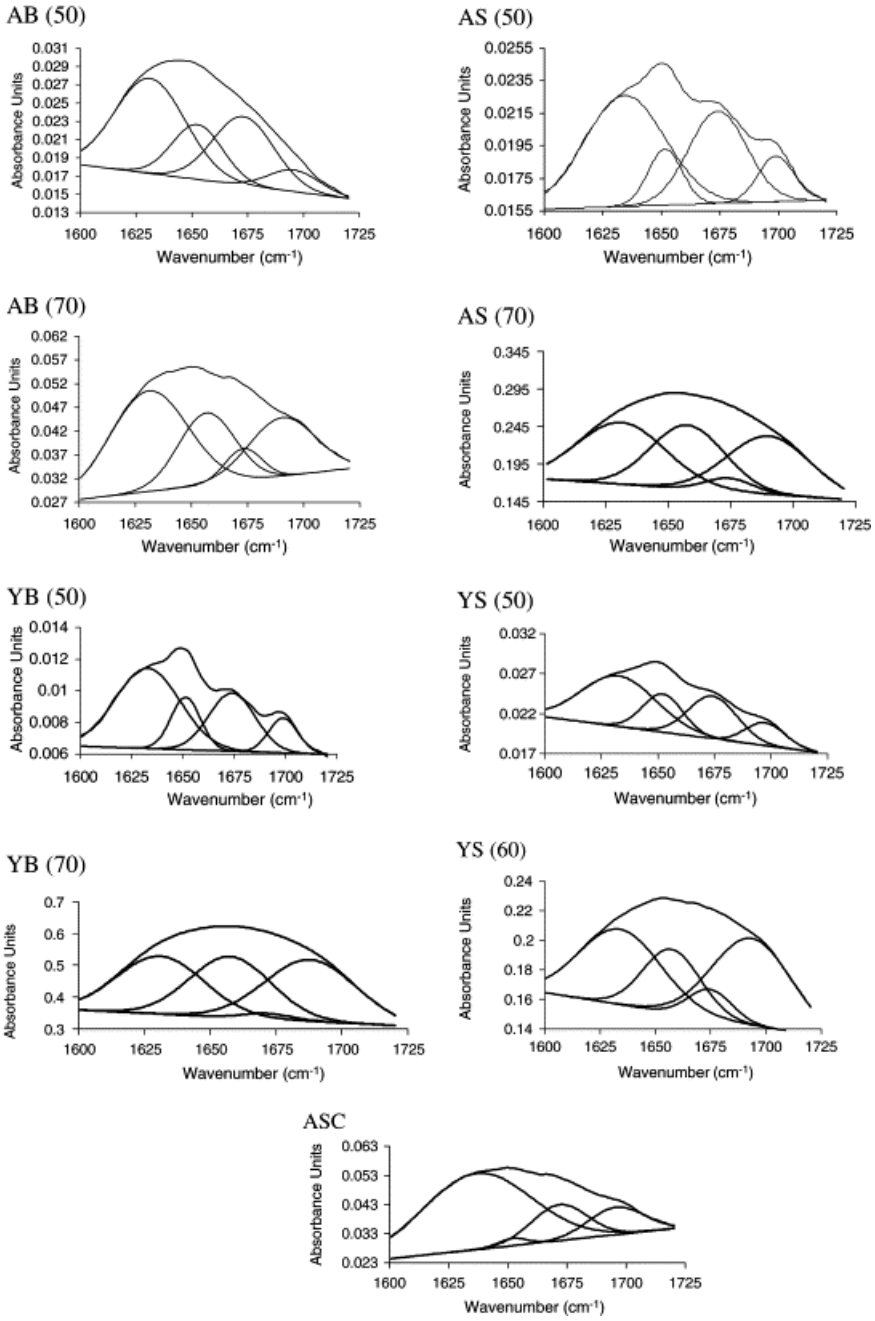

Fig. 16: Amide I band for Nile perch gelatins and collagens with fitted band components ASC – Young Nile perch skin acid soluble collagen, AB – Gelatin extracted from adult fish bones, YB – Gelatin extracted from young fish bones, AS – Gelatin extracted from adult fish skins, YS – Gelatin extracted from young fish skins. Numbers in brackets represent extraction temperature for the gelatin [57].

Muyonga with team characterised ASC from skins of young and adult Nile perch [57]. ASC was extracted from the skins of young and adult Nile perch by 0.5 M acetic acid and precipitation with 0.9 M NaCl. FTIR spectra and deconvoluted bands were obtained by method mentioned before [57], [73].

The spectra for acid soluble collagen from young and adult fish skins differed slightly, indicating some differences in the secondary structure of the two proteins. Generally, the peaks for the young fish collagen appeared at a lower frequency than the corresponding peaks for the adult fish collagen. The amide I and amide II peaks were at a lower frequency for the young fish skin (1 650 and 1 542 cm^{-1}) than the adult fish skin (1 654 and 1 555 cm^{-1}) collagen. Based on the location of the amide I and amide II peaks, it would seem that the acid-soluble collagen from the young skins had a lower degree of molecular order, since a shift of these peaks to lower wave numbers is associated with a decrease in the molecular order [57], [77]. It would appear, that there were more intermolecular cross-links in the adult fish collagen. Amide I components (Fig. 17) showed adult Nile perch ASC amide I band to consist of a higher proportion of the component at 1 695 cm^{-1} than the young fish ASC. This band is linked to the extent of intermolecular interactions in collagen and collagen-like peptides [56]. The other considerable difference was the lower intensity of the component with a peak at 1 652 cm^{-1} in young fish ASC [57]. This component has been attributed to random coils [57], [76], suggesting a lower extent of unwinding of the triple helix in the young fish ASC. It seemed, that adult fish ASC retained more intermolecular cross-links during solubilisation with acetic acid but the triple helical structure was extensively destroyed. The young fish ASC on the other hand, because of its lower content of stable intermolecular bonds, could be solubilised more easily and perhaps retained triple helices to a greater extent. The minimal differences in the extent of collagen cross-linking with age were therefore reflected in differences in the FTIR spectra of the collagens [57].

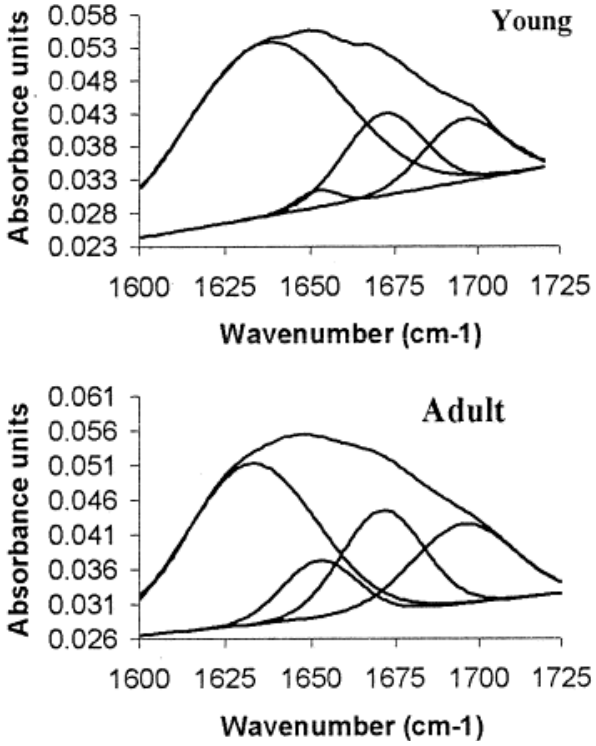

Fig. 17: Deconvoluted amide I bands for collagens from the skins of young and adult Nile perch [73].

3 GOAL OF THE WORK

1. Theoretical part-collagen and characterization of its secondary structure.
2. Preparation of collagen/gelatine films, optimization of the CD method.
3. Testing various collagen samples by CD and ATR methods.
4. Evaluation and discussion.
5. Conclusion.

4 EXPERIMENTAL PART

4.1 Chemicals

Bovine Purecol – Collagen type I, c = 3.1 mg/ml (Advanced Biomatrix),
HCl – 35 % p. a. (Lach-ner),
H_2SO_4 – 96 % p. a. (Penta),
H_2O_2 – 30% p. a. (Penta),
Acetone – 99.5 % p. a. (Penta),
Isopropylalkohol – 99.8 % p. a. (Penta),
Bovine gelatine – powder, type B (Sigma),
NaOH – pearls, p. a. (Lach-ner),
N_2 – gas, purity 99.999 6 %.

4.2 Preparation of collagen solutions

Collagen mass was cut to small pieces of size 3 mm × 3 mm and placed into beaker and beaker. A certain volume of ultrapure water was added to obtain approximately 0.5% (w/w) collagen suspension. Collagen mass was left to swell for 2 h at 5 °C. Swelled suspension was mixed by disintegrator for 5 min with speed 5 000 rotation per minute (RPM) and during this process was cooled in ice bath to prevent heating and subsequent degradation of collagen. Collagen mixture was next time left to swell for 1 h and mixed again for 5 min, 5 000 RPM. Mixed collagen suspension was poured into Petri dishes and lyophilized under -45 °C for 2 days. From lyophilized collagen, solution of accurate concentration was prepared. Exact amount of lyophilized collagen was cut into small pieces and calculated amount of 0.01 M hydrochloric acid (HCl) was added. It was left to swell for 1 h and then mixed with disintegrator for 3 min with speed 4 000 RPM in ice bath.

4.3 Preparation of collagen films

4.3.1 Surface treatment of silica windows

Cleaned silica windows without any treatment are hydrophobic to collagen solution as there was remarkable high surface tension after collagen solution application. This was followed by collagen agglomeration in the middle of windows and collagen molecules formed crystalline structureduring drying process. To obtain homogenously distributed layer of collagen we need to decrease surface tension and increase wettability of silica windows. Increased wettability of silica windows was reached by these 2 methods:

Ultrasound

Cleaned silica windows were placed into beakers with 2% NaOH solution. Beakers with windows were placed into ultrasound without heating for 10 min. After that windows were pulled out of beakers, rinsed with pure water and dried. Windows were placed into beakers with isopropanol. Then beakers were placed into ultrasound without heating for 10 min. Windows were pulled out of beakers and dried by N_2 gas.

Piranha solution

Firstly piranha solution was prepared by mixing H_2SO_4 (96 %) with H_2O_2 (30 %) in ratio 3/1. Silica windows were placed into beakers with piranha solution for 10 min. Then they were pulled out of piranha solution and were 2 times rinsed in acetone to get rid of remains of piranha solution. Windows were pulled out of acetone and placed into the beakers with isopropanol. Beakers with windows were placed into ultrasound without heating for 10 min. Then they were pulled out of beakers and dried by N_2 gas.

After both methods silica windows should be stored in desiccator under inert atmosphere (N_2) or immediately used for preparation of samples.

4.3.2 Optimization of concentration of collagen for measurement

Optimized concentration is very important parameter of measuring by circular dichroism. We need to find out right concentration which will show strong signal of elipticity and at the same time low absorbtion of circulary polarized light. Also important is ensure maximal homogenity of sample through drying process which is also highly influenced by concentration of collagen.

Solutions of collagen were prepared from dissolved pure bovine collagen with exact concentration of 3.1 mg/ml (Purecol) or 10 mg/ml (Fibricol) and diluted with 0.01 M HCl. This concentration of HCl was used because of exact solutions of collagen was dissolved in the same medium. Finally 8 solutions with concentrations from 1 to 4.5 mg/ml with step 0.5 mg/ml were prepared. Then 50 μl of solutions were put down on silica windows and were dried in vacuum drying oven with pressure 0.1 atm for 2 h at 23 °C. Prepared samples were taken out of vacuum dryer and measured on CD spectrophotometer JASCO-1500 and compared.

4.3.3 Optimization of volume of collagenfor measurement

Amount of collagen solution influences thickness of collagen layer created on silica windows. Thickess of collagen layer highly influences signal of measurement (elipticity) and also absorption of circulary polarized light. These are the reasons why is neccesary to find suitable volume for preparation of samples.

Firstly, solution of collagen with concentration 2 mg/ml was prepared. Then was created volume board consisted of 5 samples. Volumes of samples were 50, 100, 150, 200 and 250 μl of solution on silica windows. They were dried in vacuum dryer with pressure 0.1 atm for 2 h at 23 °C.Then they were measured on CD spectrophotometer JASCO-1500 and compared.

4.3.4 Optimization of drying process of collagen

Drying is very important process of preparation collagen samples. Mainly aggregation and crystallization of collagen is needed to prevent. When agreggation of collagen occurs, absorbtion of circulary polarized light highly increases, so small or no signal comes to detector.

Firstly we prepared solution of collagen with concentration of 2 mg/ml. Then 50 μl of solution was put down on silica windows and were dried by these 4 methods:

- *Drying at room temperature in air atmosphere*

Prepared samples were placed into desiccator under air atmosphere for 24 h at 23 °C.

- *Drying at room temperature in inert atmosphere (N_2)*

Prepared samples were placed into desiccator under inert atmosphere (N_2) for 24 hat 23 °C.

- *Freezing samples for 30 min and then drying at room temperature in vacuum dryer*

Prepared samples were placed into freezer for 30 min. Freezed samples were placed into vacuum dryer with pressure 0,1 atm for 2 h at 23 °C.

- *Drying at room temperature in vacuum dryer*

Prepared samples were placed into vacuum dryer with pressure 0,1 atm for 2 h at 23 °C.

After drying process all samples were measured on CD spectrophotometer JASCO-1500 and compared.

4.3.5 Calibration line for collagen/gelatine ratio

From previous results Piranha solution treatment procedure for silica windows was chosen. Solutions of collagen/gelatine with concentration of 2 mg/ml in 0.01 M hydrochloric acid were prepared. Percentage ratios of collagen/gelatine in solutions were 100/0, 85/15, 75/25, 60/40, 50/50, 35/65, 20/80 and 0/100. 50 μl of every solution was dosed on modified silica windows and dried in vacuum dryer for 2 h at 23°C. Then they were taken out and measured on CD spectrophotometer JASCO-1500.

4.4 Measuring of collagen samples by CD spectroscopy

4.4.1 Parameters

For measuring of CD was used spectrophotometer JASCO-1500. Before the measurement right parameters was set. Wavelenght measurement was set between 180 and 250 nm, which was also used in quotations [14], [28]. Data pitch was set to 2 nm. Scanning speed was set to 50 nm/min and bandwidth to 3.0 nm. There were measured 2 channels, first one for CD signal in milidegree (mdeg) and second one for absorbance (HT) in volts (V). All obtained data were evaluated in program Spectra Analysis.

4.4.2 Evaluation

Baseline for each clear silica windows was measured. Clear silica windows exibited absorption (HT) of circulary polarized light (Fig. 18), which is caused by attached H_2O to the surface molecules of SiO_2. It is comfirmed by rapid increasing values of HT from 190 nm, which is caused by high absorbance of H_2O molecules. To find out true absorbtion of collagen films, the absorption of surface attached H_2O molecules was substracted (4). HT absorbtion of films cannot pass over 600 V, because then signal which comes to detector is not satisfying what cause that results are not reproducible [4].

$$HT\ (films)\text{-}HT\ (windows)=HT\ (sample) \qquad (4)$$

Resulting value of circular dichroism for collagen films was calculated as compensation of ellipticity divided by HT (sample) (5).

$$\theta/HT\ (sample)=compensation \qquad (5)$$

Every collagen film was measured 3 times with different rotation (0°, 45° and 90°) and then calculated average of them.

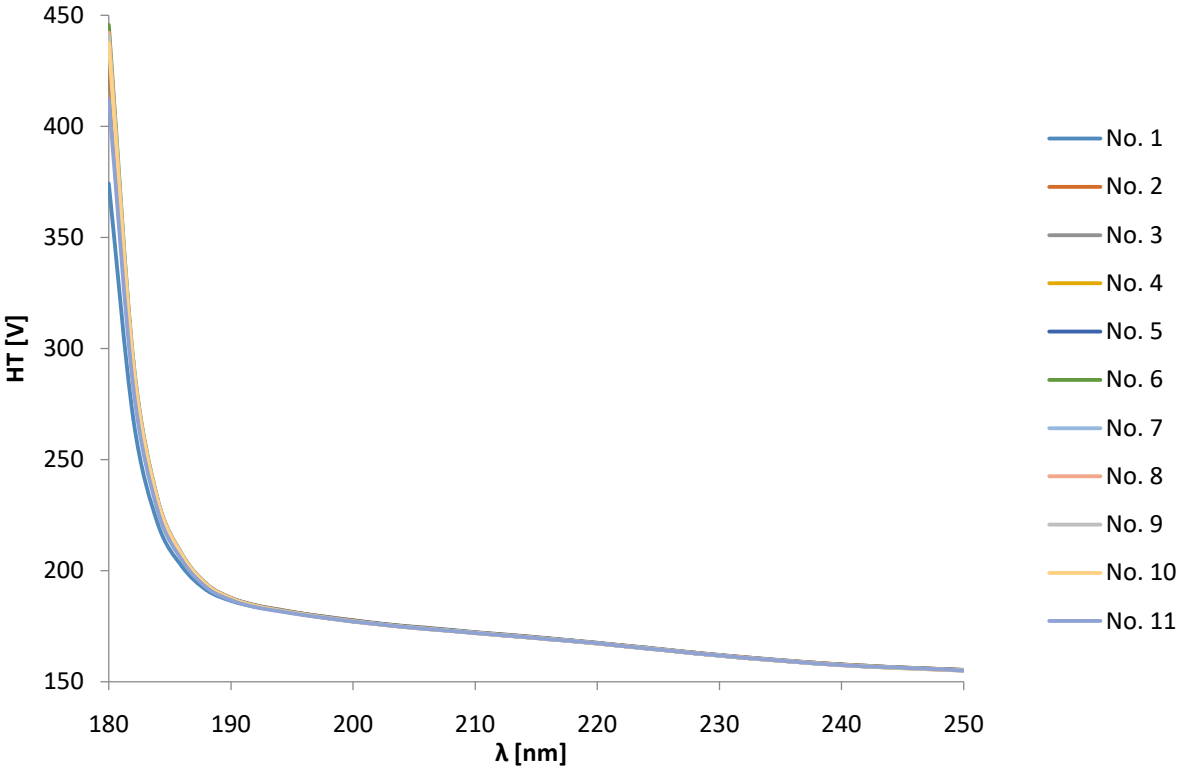

Fig. 18: Dependance of HT signal on wavelength of cleaned silica windows.

4.5 Measuring of collagen samples by ATR spectroscopy

Samples were measured by ATR. Firstly we setted parameters for measument. Wavenumber was set from 4 000 to 800 cm^{-1}. Samples were scanned 32 times with resolution 4 cm^{-1}. Background was measured without sample and with evacuated chamber. Then chamber was vented and small piece of lyophilized samples were cut and placed on germanium crystal of spectrophotometer. Samples were pressed on crystal and chamber was evacuated. Samples were measured and taken out of chamber. Every sample was measured 5 times, and every cut was taken from different part of lyofilized sample. After meassurement infrared spectra were evaluated in OPUS 7.5.

5 RESULTS AND DISCUSSION

5.1 Preparation of collagen films

5.1.1 Optimization of concentration of collagen for measurement

Collagen films of different concentrations were prepared by method mentioned before. Fig. 19 displays prepared films look like. In the range of concentrations 1 – 2.5 mg/ml (Fig. 18 a-d), no visible difference was observed. All of them are thin and transparent films. In comparison with films in Fig. 19 e-h they are more homogenous. In Fig. 19 e-h, there are noticeable nonhomogenous artefacts, which were formed during drying process. Collagens with higher concentrations then 2 mg/ml were too dense and bubbles which was formed in collagen during drying process had no time to escape and created damaged layer of film.

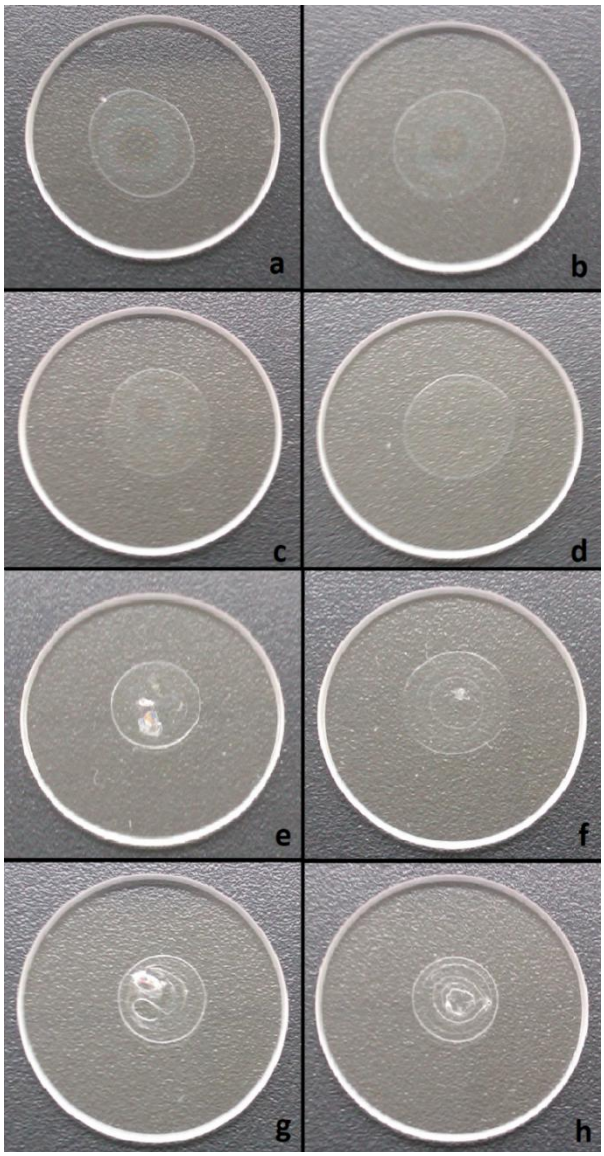

Fig. 19: Prepared collagen films with concentration 1 mg/ml (a), 1.5 mg/ml (b), 2 mg/ml (c), 2.5 mg/ml (d), 3 mg/ml (e), 3.5 mg/ml (f), 4 mg/ml (g) and 4.5 mg/ml (h).

Collagen films were measured by CD on JASCO-1500 spectrophotometer. Measured wavelegth was between 180 and 250 nm. The results are shown in Fig. 20. Ellipticity of samples with concentration 1.0 – 2.5 mg/ml (Fig. 20 (a)) had positive peaks around 230 nm. It is probably signal of triple helical structure of collagen. Samples with concentration between 3.0 – 4.5 mg/ml had mostly negative peaks. It was caused by higher absorbtion of circularly polarized light (Fig. 20 (b)) and agglomeration of small collagen particles. Aglomerates probably created structures, whose are responsible for negative peaks in all samples with higher concentration then 2.5 mg/ml. Samples with concentration of 1.0 and 1.5 mg/ml had positive peaks, but their signal was too weak for accurate evaluation. This was due to a small amount of particles that produce signal. The best results were reached with samples of concentration 2.0 and 2.5 mg/ml. These two samples had optimal amount of particles in solution what means relatively low absorbtion and still high signal of circularly polarized light.

Solution of collagen with concentration 2 mg/ml was chosen for the next measurements.

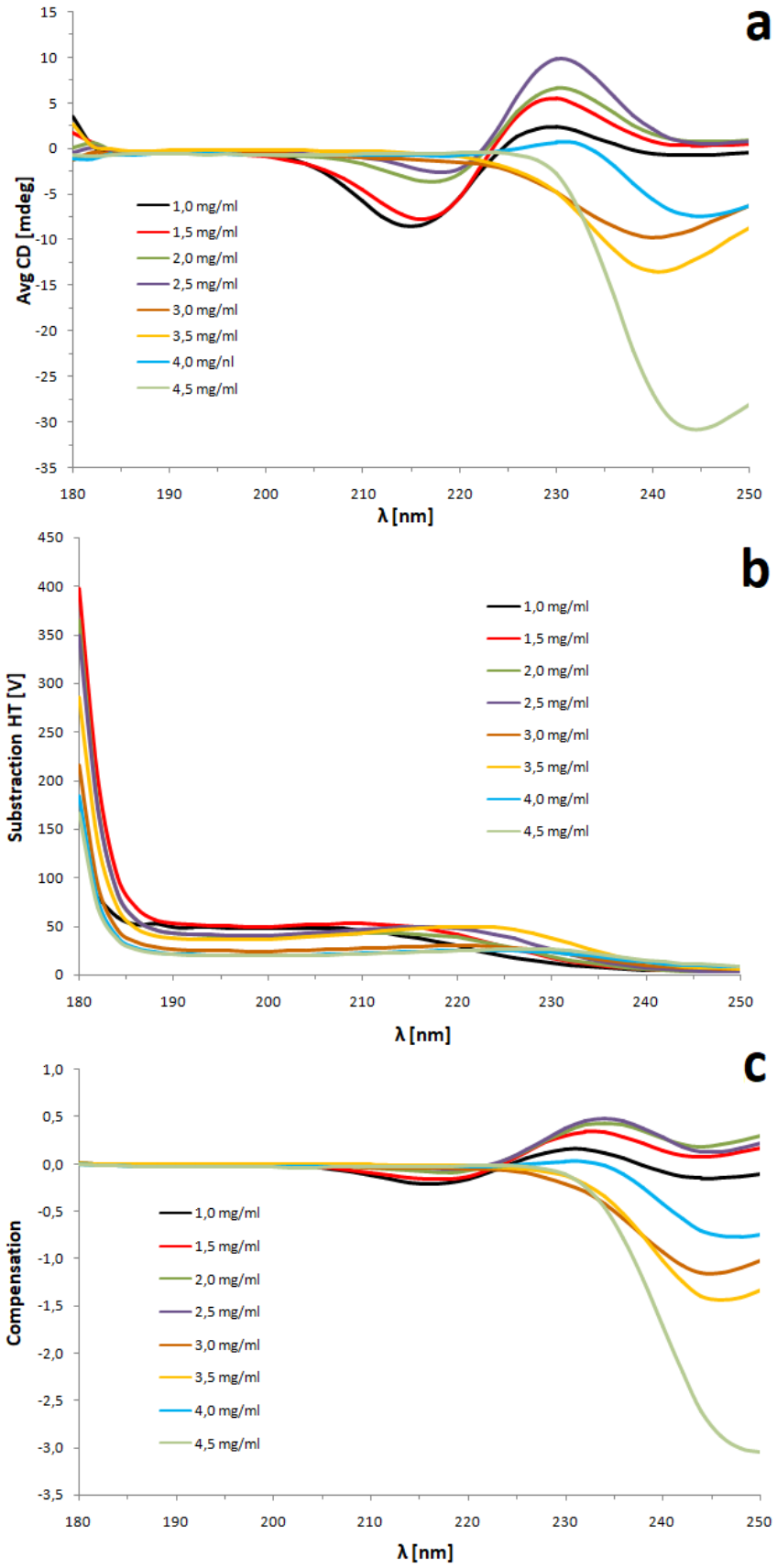

Fig. 20: Measured dependence of ellipticity on wavelength (a), calculated dependence of substraction HT on wavelength (b) and calculated dependence of compensation on wavelength (c) of samples with different concentrations.

5.1.2 Optimization of collagen solution volume for measurement

Collagen films with different volumes (50, 100, 150, 200 and 250 μl) of collagen solution were prepared by method mentioned before. Fig. 21 shows prepared collagen films. Sample with 50 μl volume (Fig. 21 (a)) is the only fully transparent and mostly homogenous. Sample with 100 μl is also transparent but not homogenous, because a bubble was created in collagen film during drying process. Samples with 150, 200 and 250 μl are neither transparent nor homogenous. This is probably caused by agglomeration of collagen in the center of silica window through process of drying. Agglomeration of collagen appeared because of slower drying caused by higher volume of collagen solution.

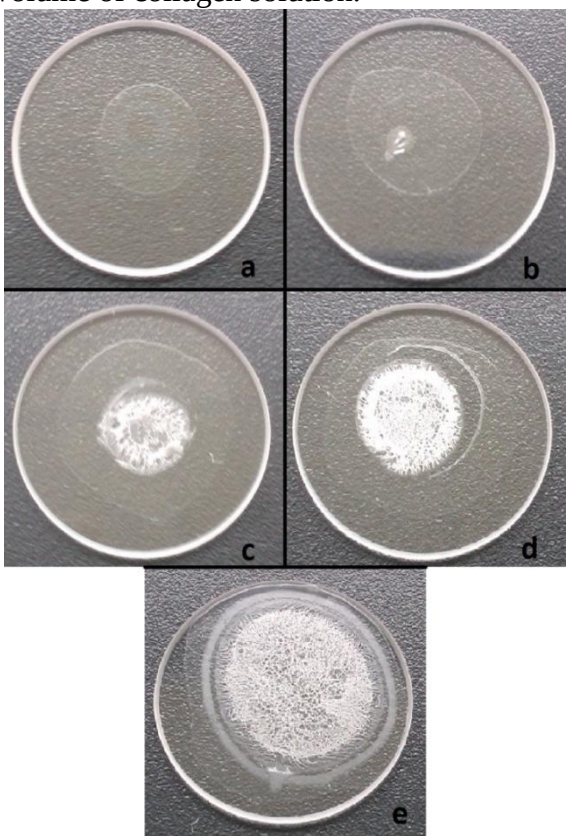

Fig. 21: Prepared collagen films with volume 50 μl (a), 100 μl (b), 150 μl (c), 200 μl (d), 250 μl (e).

Collagen films were measured by CD on JASCO-1500 spectrophotometer at wavelegth between 180 and 250 nm. The results are shown in Fig. 22. The highest ellipticity signal was reached by sample with volume of 150 μl (Fig. 22 (a)). This sample contains enough particles for CD signal and do not crystallized during drying process. Samples with volume 200 and 250 μl had the lowest signal. Too large volumes of collagen solution used in these 2 samples caused long lasting drying process which gave rise to their agglomeration. Agglomerates absorb source polarized light too much, so there almost no signal comes to detector. The highest compensation was calculated for sample 50 μl. Althought the sample with 150 μl had the highest ellipticity signal, it had also the highest absorbance of polarized light (Fig. 22 (b)) what caused that calculated resulting compensation was low (Fig. 22 (c)). Sample with volume 50 μl had lower ellipticity signal with comparison to sample with 150 μl, but absorbed the source light much less so the resulting compensation was the highest of all samples.

For the next measurements volume 50 μl of collagen solution for film preparation was chosen.

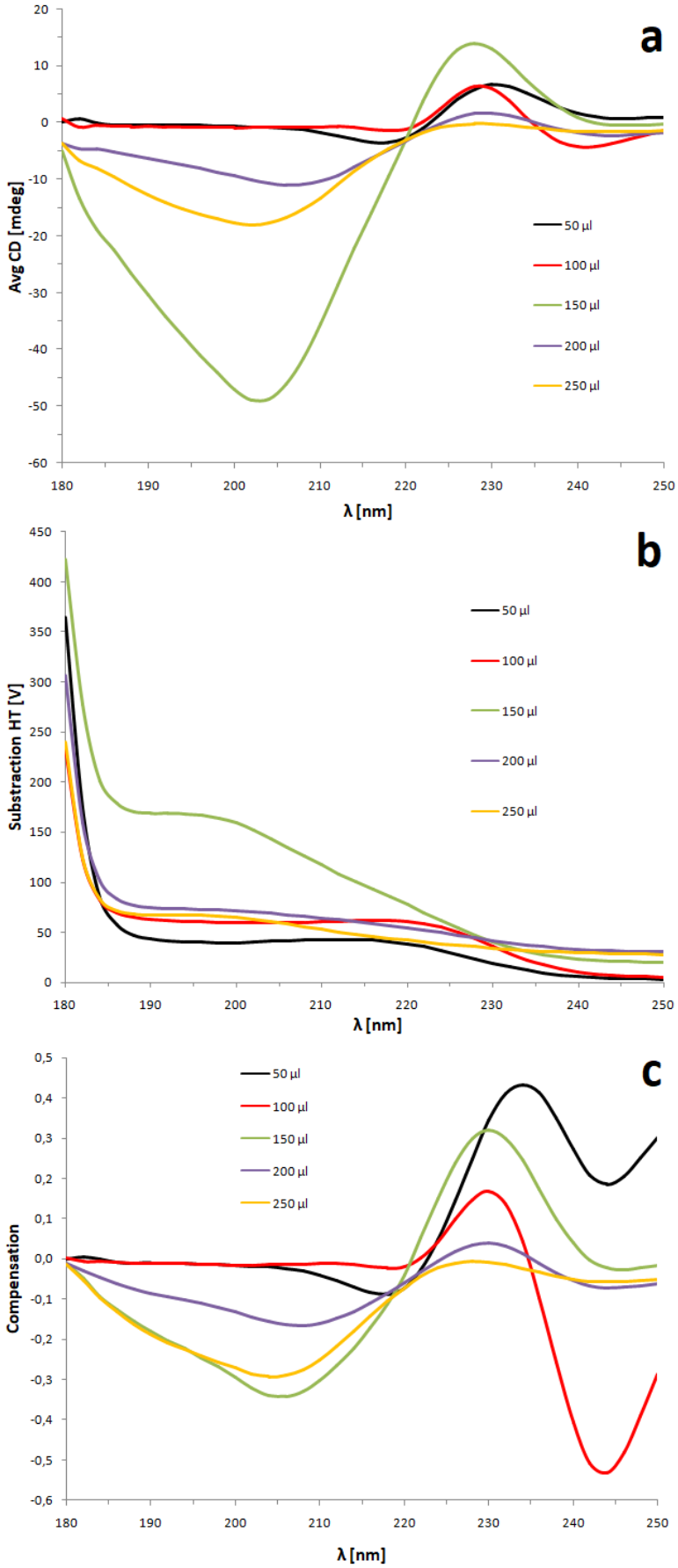

Fig. 22: Measured dependence of ellipticity on wavelength (a), calculated dependence of substraction HT on wavelength (b) and calculated dependence of compensation on wavelength (c) of samples with different volume.

5.1.3 Optimization of drying process of collagen films

Collagen films with concentration 2 mg/ml and volume 50 µl were prepared by method mentioned before. They were dried by different methods and then compared. The film prepared by drying in desiccator under air atmosphere for 24 h (Fig. 23 (a)) created small spherical film with white non-transparent dot in the center. White dot is agglomerate of collagen, which is caused by too long time of drying. Collagen had enough time to transport in solution and created agglomerates during drying process. The film prepared by drying in desiccator under nitrogen atmosphere for 24 h (Fig. 23 (b)) looks similar to the first one. There were agglomerates of collagen in the centre of sample as well. From this statement, nitrogen atmosphere did not influence or stop agglomeration of collagen. Film prepared by drying in vacuum dryer for 2 h at 23 °C with previous freezing for 30 min (Fig. 23 (c)) created transparent layer of collagen. The best film was created by drying in vacuum dryer for 2 h at 23 °C with no previous freezing of sample (Fig. 23 (d)). This film showed as the most transparent and homogenous. All methods of drying are summarized in Tab. 3.

Tab. 3: Summary of all methods of drying samples.

Method	Desiccator	Gas	Vacuum dryer	Freezing
A	+	air	-	-
B	+	N_2	-	-
C	-	-	+	+
D	-	-	+	-

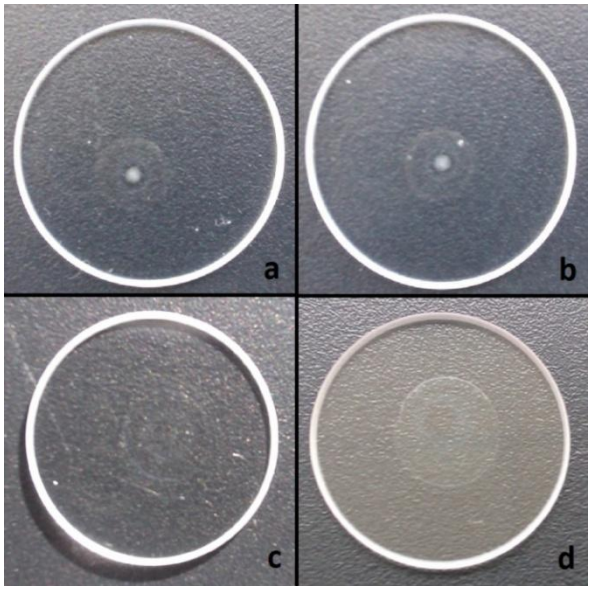

Fig. 23: Prepared collagen films with concentration 2 mg/ml and volume 50 µl dried in desiccator under air atmosphere for 24 h (a), dried in desiccator under N_2 atmosphere for 24 h (b), freezed for 30 min and dried in vacuum dryer with pressure 0.1 atm for 2 h at 23 °C (c), dried in vacuum dryer with pressure 0.1 atm for 2 h at 23 °C (d).

Collagen films were measured by CD on JASCO-1500 spectrophotometer at wavelegth between 180 and 250 nm. The results are shown in Fig. 24. Samples prepared in desiccator with air and nitrogen atmosphere (method A and B) showed no positive peaks. Again, it may be caused by agglomeration of collagen in the middle of sample. Agglomeration took place because of too long lasting process of drying, when collagen chains had enough time to transport and create structure responsible for negative peaks in both samples. On the other hand collagens dried in vacuum dryer had positive peaks. It means that they were dried fast enough to prevent agglomeration. Samples prepared by method C and D differedin freezing procedure before drying process which caused change in results of ellipticity signal and absorbance. Sample prepared by method C had higher ellipticity signal, but also higher absorbance of circularly polarized light. In Fig. 24 (c) is shown, that better ratio between ellipticity and absorbance reached sample prepared by method D. Freezing probably prevent collagen agglomeration what caused higher ellipticity signal was obtained. However previous freezing of sample also influenced or rebuilt structure of collagen, what caused many times higher absorbance.

For the next measurements drying method D (in vacuum dryer without freezing) was chosen.

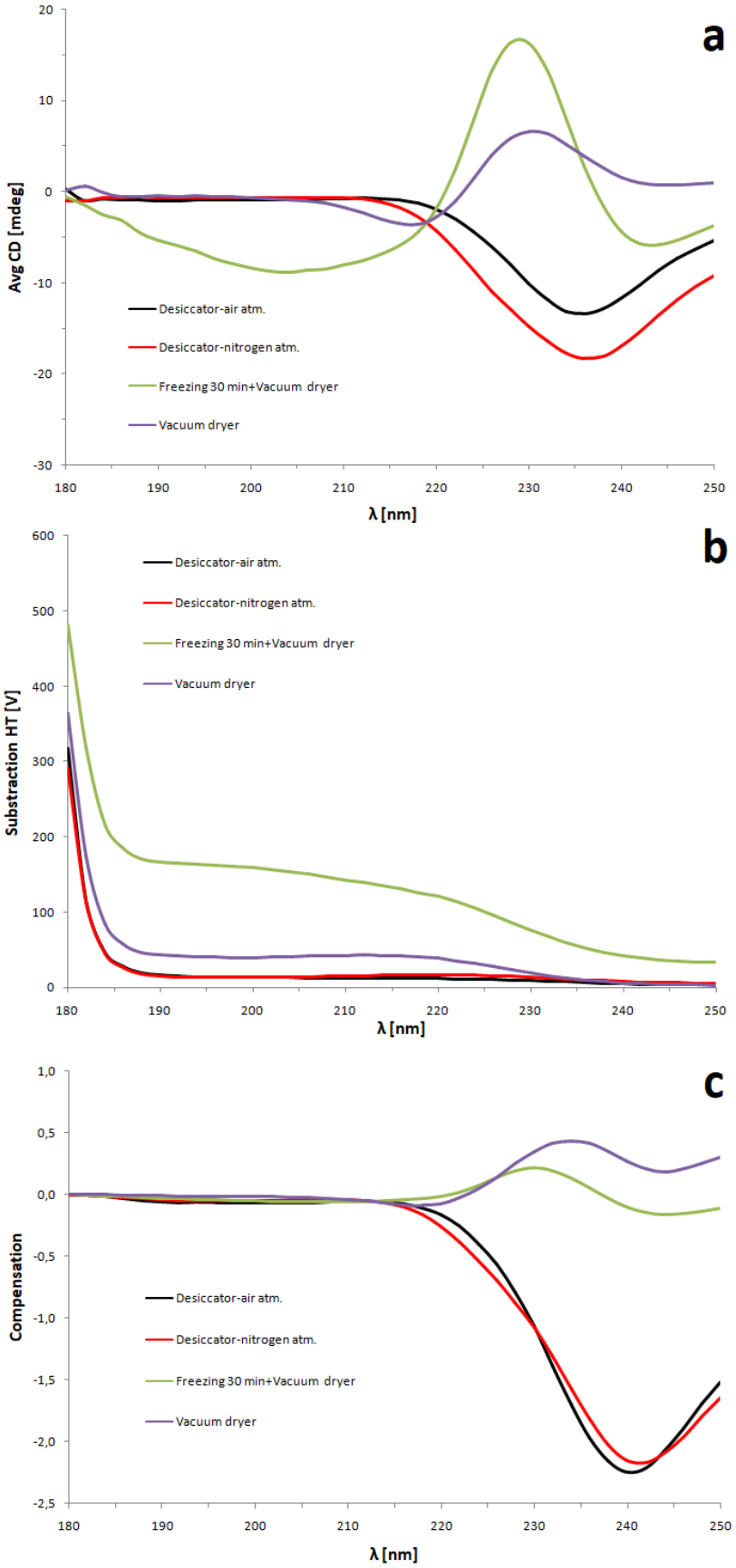

Fig. 24: Measured dependence of ellipticity on wavelength (a), calculated dependence of substraction HT on wavelength (b) and calculated dependence of compensation on wavelength (c) of samples with different drying process.

5.1.4 Calibration line for collagen/gelatine ratio

Collagen/gelatine films with concentration 2 mg/ml and volume 50 μl were prepared. They were measured by CD on JASCO-1500 spectrophotometer at wavelegth between 180 and 240 nm. Average ellipticity signal of every sample is shown in Fig. 25 (a). All samples displays peak around 230 nm. The lowest ellipticity signal was measured for sample of pure gelatine. It comfirmed, that pure gelatine had the lowest organization of chains. Positive peak in 230 nm grew up with increasing amount of collagen in sample. This claim cannot be applied for sample with 100 % of collagen. 100% collagen presents a little decrease in ellipticity signal. Pure collagen without gelatin tends to form crystals from chains which are not fully transparent. Crystallization of collagen did not occur in other samples because they were widespread between gelatine chains, which probably stopped this process.

In Fig. 25 (b) there are calculated absorbances (substraction HT) of samples without silica windows. Just sample with 100 % of gelatine showed little bit higher absorbance caused by low transmissivity of gelatine chains. Compensations of collagen/gelatine mixtures were calculated from ellipticity signal and absorbance (Fig. 25 (c)). From values of compensation at 230 nm calibration line was created (Fig. 26). Calibration line was also edited to start from zero, because not all values were positive. Only sample with 100% of collagen was no included to calibration line, because of lower compensation, which is caused by lower ellipticity signal of sample explained before. From calibration line, the linear regression was obtained, which was used for determining the amount of collagen in modified samples.

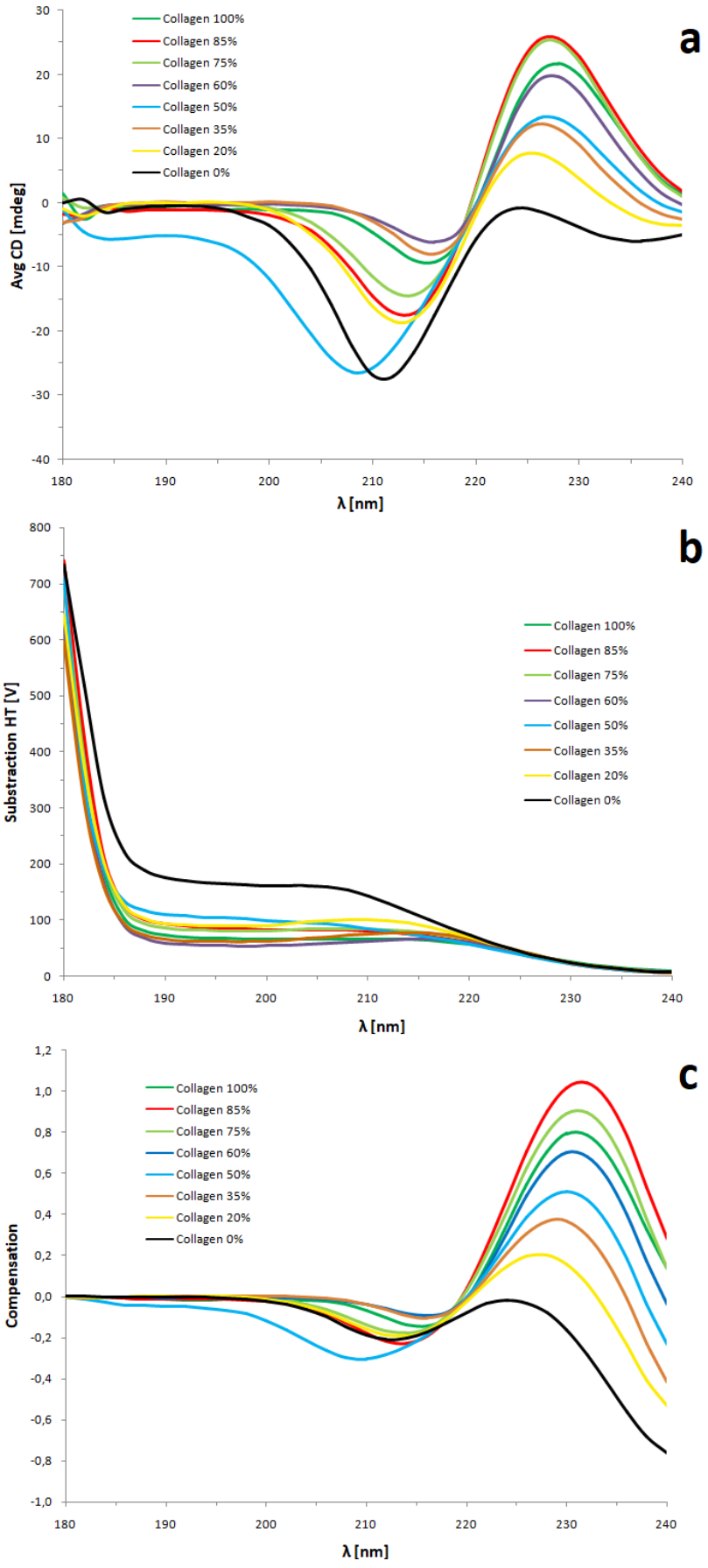

Fig. 25: Measured dependence of ellipticity on wavelength (a), calculated dependence of substraction HT on wavelength (b) and calculated dependence of compensation on wavelength (c) of calibration line.

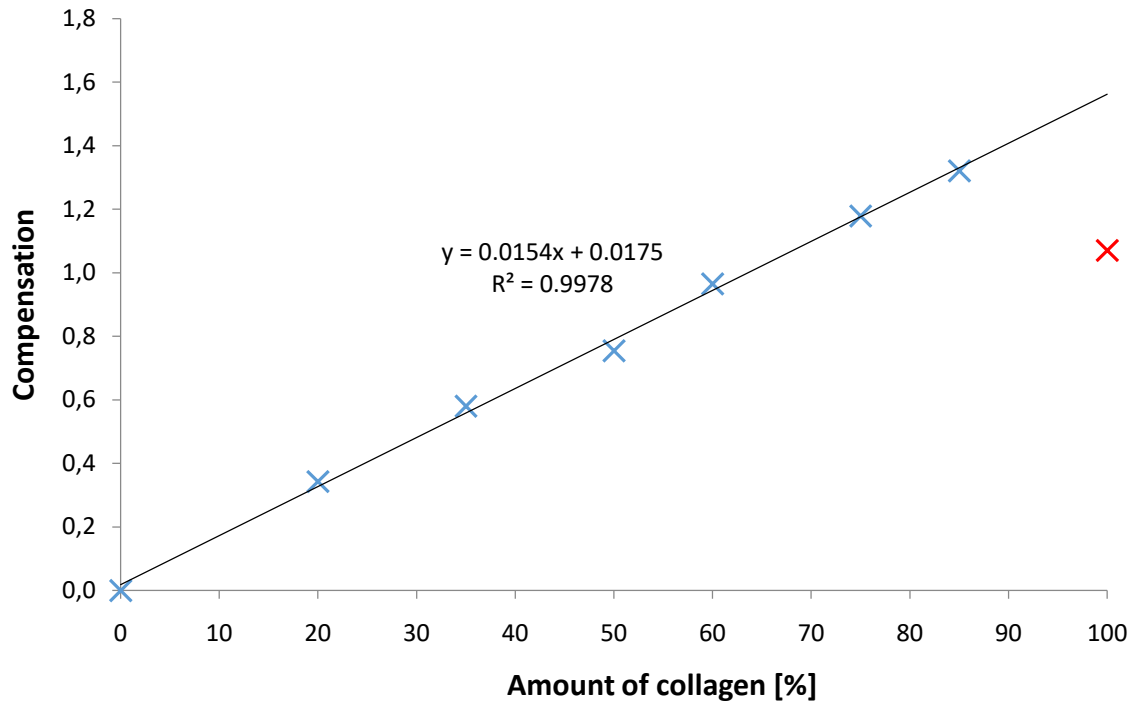

Fig. 26: Calibration line dependence of compensation on amount of collagen.

5.2 Measurement of modified samples

5.2.1 Measurement of modified samples by CD spectroscopy

Collagen mass with around 35 % of collagen was exposed to different conditions (Tab. 4). Changes in contents of collagen were observed. Sample 3 was mixed for 45 min and gradually heated to 28 °C. Sample 4 was mixed for 45 min at 10 °C. Sample 6 was mixed for 90 min and gradually heated to 37 °C. Sample 8 was mixed for 20 min and rapidly heated to 37 °C. Sample 11 was mixed for 180 min at 10 °C. Sample 12 was mixed for 20 min and gradually heated to 20 °C. Sample 14 was mixed for 45 min and gradually heated to 32 °C.

Tab. 4: Samples prepared under different conditions.

Sample No.	3	4	6	8	11	12	14
Mixing time [min]	45	45	90	20	180	20	45
Temperature [°C]	28	10	37	37	10	20	32

From samples were prepared solutions (method mention before) with concentration of 2 mg/ml. 50 µl of every solution were 3 times dosed on silica windows and dried in vacuum dryer for 2 h at 23 °C. Every sample was 3 times measured by CD on JASCO-1500 spectrophotometer. Measured wavelegth was between 180 and 240 nm.

Average ellipticity of samples is displayed in Fig. 27 (a). All samples shows positive peak in location around 230 nm. It means that in every sample is certain amount of collagen presented. The lowest signal was measured for samples 6 and 8. It was mainly caused by heating to temperature 37 °C, which caused denaturation of collagen to gelatine. Sample 8 was a little bit higher then 6 because it was heated rapidly so collagen had no equal time to denaturate as sample 6. Higher ellipticity signal got samples 3, 4 and 14. These samples were slightly influenced by exposed conditions. All of them was mixed for 45 min what proves that collagen in samples was not influenced by this time of mixing. Different heating of these 3 samples did not caused significant changes in ellipticity signal. The highest signal reached samples 11 and 12. Both of them refered, that they are not denaturated. They had also slightly higher signal then original collagen mass. For sample 11, it was caused by long lasting mixing, which caused cutting of collagen to smaller particles. Lower distribution of particles seems to be important for measurements on circular dichroism spectroscopy. Values of absorbance differ just slightly what means that calculated compensations are almost the same as measured values of ellipticity.

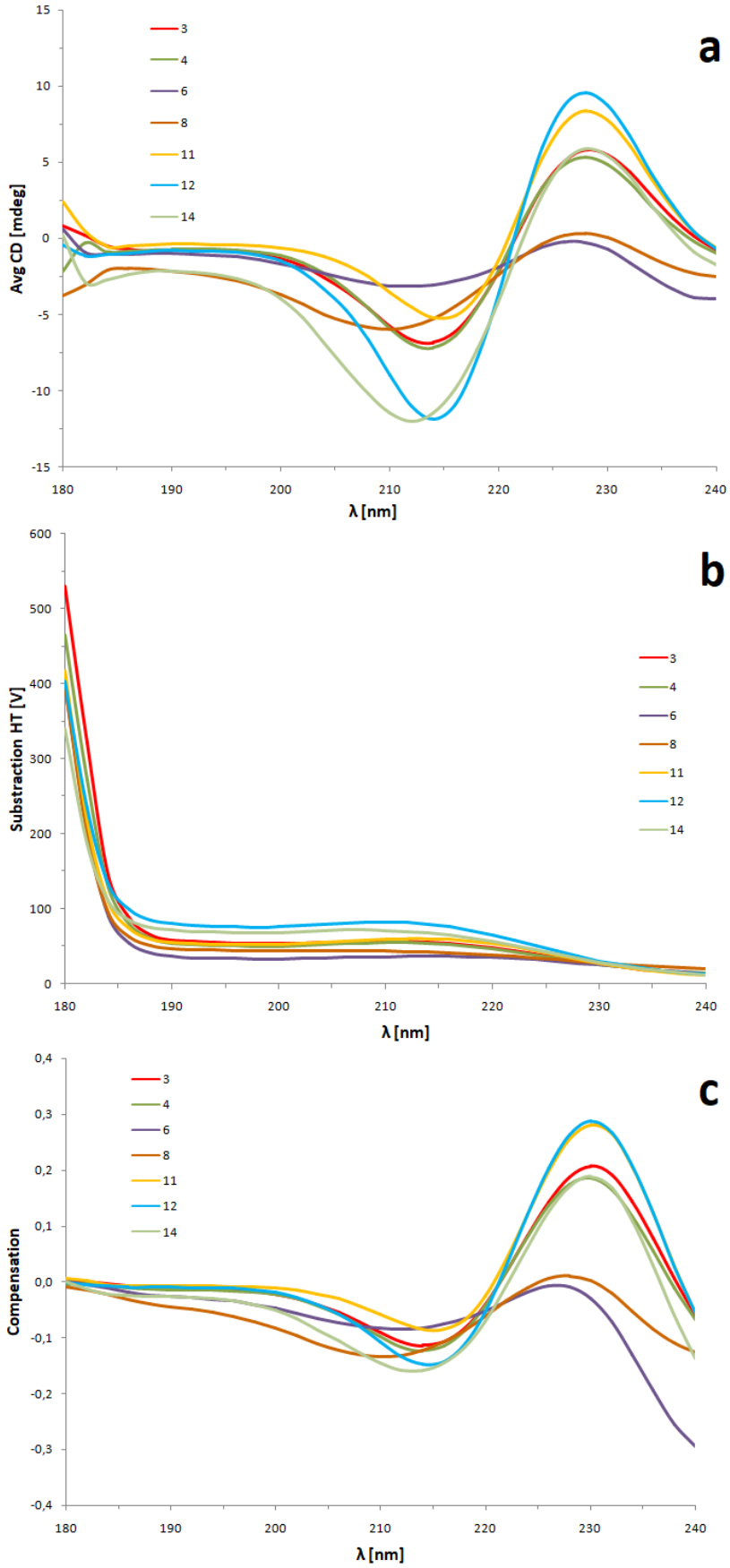

Fig. 27: Measured dependence of ellipticity on wavelength (a), calculated dependence of substraction HT on wavelength (b) and calculated dependence of compensation on wavelength (c) of modified samples.

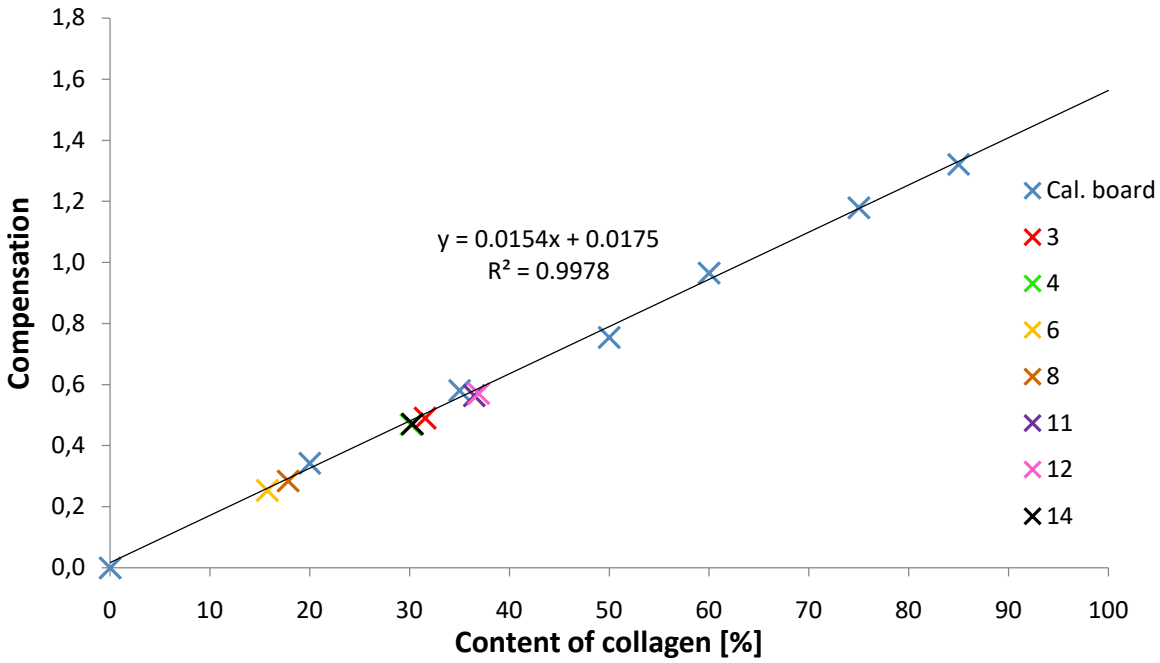

Fig. 28: Modified samples placed to calibration line.

From all modified samples values of compensations in 230 nm were chosen. Values were put to calibration line (Fig. 28) and by using of linear regression equation amount of collagen in percentage was calculated. Calculated values are represented in Tab.5.

Tab.5: Results of modified samples.

Sample	3	4	6	8	11	12	14
Content of collagen [%]	31.6	30.1	15.8	17.8	36.5	36.9	30.3

Samples 3, 4 and 14 were mixed for 45 min. They differ only in heated temperature. All 3 samples show almost the same collagen content. It was caused by low temperature (10 °C) during mixing. On the other hand samples 3 and 14 showed lower collagen contents. It was caused by heating of these 2 samples (28 °C for sample 3 and 32 °C for sample 14) which caused denaturation of collagen parts. From all samples, the lowest collagen contents were calculated for samples 6 and 8. These samples were heated until 37 °C. Both samples were highly denatured. In sample 6 collagen content was slightly lower with comparison to sample 8. It was caused by diferent speed of heating. Sample 6 was heated gradually for 90 min so it had more time to denaturate then sample 8 which was heated rapidly for 20 min. The highest collagen content were reached by samples 11 and 12. Sample 11 was only mixed for 180 min at 10 °C and sample 12 was gradually heated to 20 °C and mixed for 20 min. In both samples denaturation of collagen did not occurs, because their temperatures are too low for denaturation.

To conclude mixing procedure had a little effect on collagen denaturation. Denaturation of collagen occurs mainly in samples heated over 28 °C. From this point, with increasing temperature the portion of collagen part is decreasing.

5.2.2 Measurement of modified samples by ATR spectroscopy

Collagen mass with around 35 % of collagen was exposed to different conditions. Changes in contents of collagen were observed. All modified samples were measured on ATR 5 times by method mentioned before. In Fig. 29 is showed example of spectra for sample 3.

The amide A peak was observed at 3 323 cm^{-1}. It represents N–H stretching vibration. N–H stretching vibration ranges from 3 400 to 3 440 cm^{-1}. In these wavenumbers amide group of a peptide was associated with a hydrogen bond [56]. The amide B peak was associated with the asymmetrical stretching of CH_2 [57]. It was situated at 2 932 cm^{-1}. The peak of amide I was located around 1 660 cm^{-1} [75]. They are associated with carbonyl group stretching vibrations and are also characteristic for secondary coil structure [16]. This observation confirmed that the hydrogen bonds between the amide group and the carbonyl group were responsible for the triple helical structure [59]. The peak of amide II was found around 1 550 cm^{-1}, while the peak of amide III was located at 1 238 cm^{-1}. The peak of amide II is connected to N–H bending vibrations, and the peak of amide III represented C–H stretching [49]. The amide III peak comfirmed the presence of a helical structure [61].

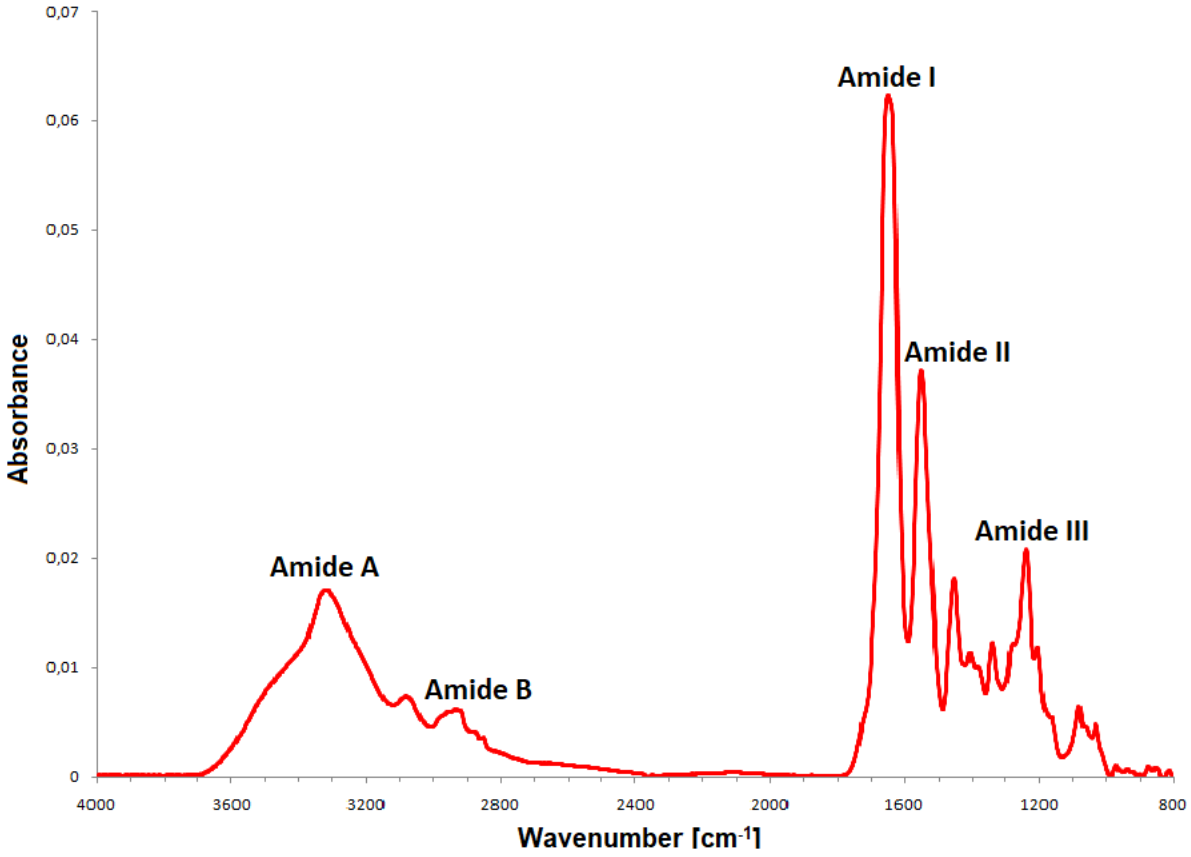

Fig. 29: Example of spectra for sample 3.

The amide I peak which is situated around wavenumber 1 660 cm^{-1} was chosen (Fig. 30). Peak was deconvoluted in range 1 750 – 1 600 cm^{-1}. In this range were found out 4 peaks, that created amide I peak. These peaks were located at wavenumbers 1 688 – 1 682 cm^{-1}, 1 660 cm^{-1}, 1 645 cm^{-1} and 1 630 cm^{-1}. The peak found in 1 688 – 1 682 cm^{-1} belongs to helices aggregated collagen like peptides, peak situated in 1 660 cm^{-1} shows a presence of triple helix, the peak placed in 1 645 cm^{-1} belongs to random coil and the peak positioned in 1 630 cm^{-1} is known as peak of gelatine [57], [73]. Peaks of gelatines, random coils and helices of aggregated collagen like peptides are denaturated parts and belong to non-collagenous part. Peak of triple helix belongs to collagenous part.

Amide I peak of every measured sample was deconvoluted and areas of deconvoluted peaks were calculated. From total area of peak amide I was calculated percentage contents of every deconvoluted peak. Peaks of non-collagenous parts (helices of aggregated collagen like peptides, random coils, gelatines) were then summed and made up gelatine part of content. Peak of collagenous part (triple helix) made up collagen part of content. Contents of collagen and gelatine in samples are shown in Tab. 6.

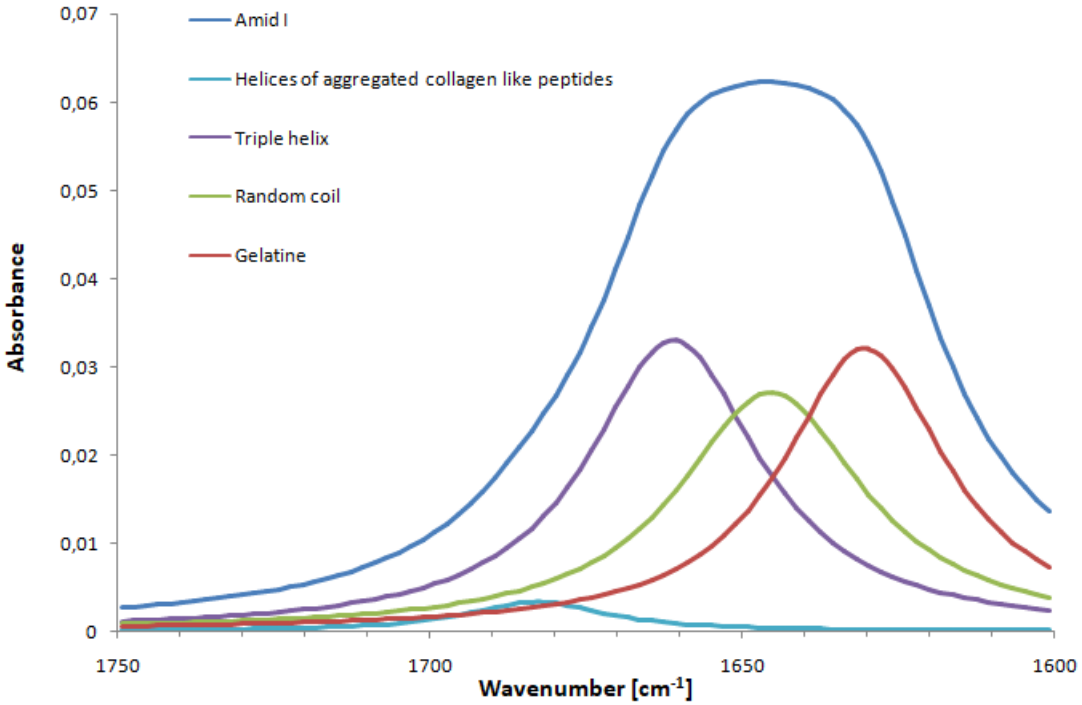

Fig. 30: Example of deconvoluted peak amide I represented on sample 3.

Tab. 6: Presence of collagen and gelatine in samples.

3		4		6		8	
Collagen [%]	Gelatine [%]	Collagen [%]	Gelatine [%]	Collagen [%]	Gelatine [%]	Collagen [%]	Gelatine [%]
36.6 ± 1.9	63.4 ± 1.9	40.7 ± 2.0	59.3 ± 2.0	34.1 ± 1.9	65.9 ± 1.9	35.7 ± 1.0	64. 3 ± 1.0
11		12		14			
Collagen [%]	Gelatine [%]	Collagen [%]	Gelatine [%]	Collagen [%]	Gelatine [%]		
42.3 ± 1.2	57.7 ± 1.2	43.5 ± 2.0	56.5 ± 2.0	39.6 ± 0.5	60.4 ± 0.5		

Samples 3, 4 and 14 were mixed for 45 min. They difer only in heated temperature. From these 3 samples, sample 4 had the highest collagen content. It was caused by low temperature (10 °C) during mixing. On the other hand samples 3 and 14 showed lower collagen contents. It was caused by heating of these 2 samples (28 °C for sample 3 and 32 °C for sample 14) which caused denaturation of collagen parts. From all samples, the lowest collagen contents were calculated for samples 6 and 8. These samples were heated until 37 °C. In both samples high denaturation of collagen occurs. In sample 6 collagen content was slightly lower with comparison to sample 8. It was caused by diferent speed of heating. Sample 8 was heated rapidly for 20 min so collagen had no time to denaturate as well as sample 6 which was heated gradually for 90 min. The highest collagen contents were calculated for samples 11 and 12. Sample 11 was only mixed for 180 min at 10 °C and sample 12 was gradually heated to 20 °C and mixed for 20 min. In both samples denaturation of collagen did not occurs, because their temperatures are too low for denaturation.

To conclude mixing procedure, it had no influece on collagen contents in samples. Denaturation of collagen occurs only in samples heated over 28 °C. From this point, with increasing temperature the portion of collagen part decreasing. Obtaining of exact ratios of 4 peaks represented in amide I peak is difficult. The reason is that peak of random coil can be located in range 1 657 – 1 645 cm^{-1}. For our measurements we used 1 645 cm^{-1}. Shifting peak of random coil to higher wavenumber will cause decreasing of triple helical peak and subsequently decreasing of collagen content. It is possible that calculated values of infrared spectroscopy are higher (5 – 10 %) than real ones.

5.2.3 Comparison of CD and ATR results

Results of CD and ATR measurements were evaluated and compared (Tab. 7 and Fig. 31).

Tab. 7: Comparison of CD and ATR results.

Sample	3	4	6	8	11	12	14
Content of collagen by CD [%]	31.6	30.1	15.8	17.8	36.5	36.9	30.3
Content of collagen by ATR [%]	36.6	40.7	34.1	35.7	42.3	43.5	39.6

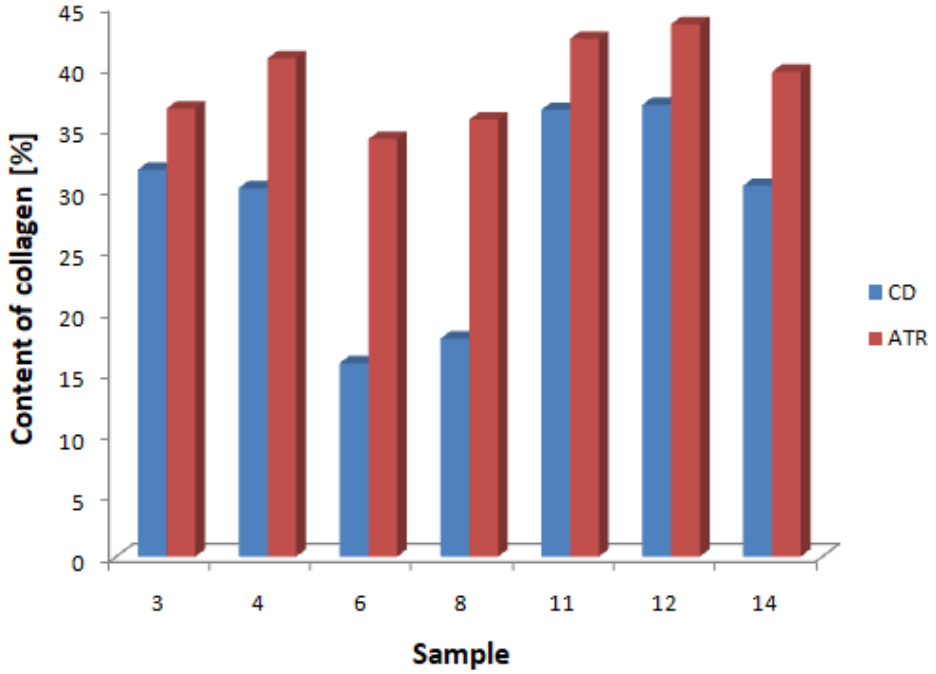

Fig. 31: Comparison of results obtained by methods CD and ATR.

In all modified samples values of ATR measurements show higher collagen content then values of CD measurements. It is caused by partial inaccuracy of ATR method (mentioned before). However there are also similarities. In both methods the lowest collagen contents were obtained for samples 6 and 8 and the highest values were reached by samples 11 and 12. It proves that samples heated at 37 °C (6 and 8) were the most denaturated and samples 11 and 12 were the least denaturated. Individual methods also shows almost the same diference between sample heated gradually (6) and sample heated rapidly (8).

The greatest difference between compared methods was in samples 6 and 8. It was caused by mentioned problem with peak of random coil which can be located in range 1 657 – 1 645 cm^{-1}. This small diference in wavenumber can cause large diference in area of peaks and subsequently in ratios of collagenous and non-collagenous parts.

To compare these 2 methods, more accurate results are obtained by CD, because there is no problem with localization and deconvolution of peaks. In CD is important only intensity of one positive peak located at 230 nm, from which we can find out collagen content of samples. However CD method is slower and more complicated because it needs accurate samples preparation under same conditions and set CD spectrophotometer correctly. Measuring collagen contents with ATR method is much easier and faster method, because samples do not need to be treated. However this method is only for approximate results.

It is very important to mention, that all results are only valid for bovine collagen and any other type of collagen will need new preparation process and calibration line with completely different results.

6 CONCLUSION

Sample preparation method for measurement of CD spectroscopy in solid phase was optimized. Transparent, homogenous films with the highest CD compensation were reached with solution concentration of 2 mg/ml, volume of 50 μl and drying in vacuum dryer for 2 h at 23 °C. Optimized preparation method was used for creation of calibration line with different ratios of collagen/gelatine. From calibration line linear regression equation was obtained. Then modified samples with unkown content of collagen/gelatine ratios were prepared and measured. Linear regression equation was used for calculation of collagen/gelatine contents in samples.

All modified samples were also measured by ATR spectroscopy. Measured spectra of modified samples were evaluated by deconvolution of amide I peak. Collagen/gelatine contents were calculated by integration of collagenous (triple helix) and non-collagenous (helices of aggregated collagen like peptides, random coils, gelatines) peaks.

Results of both methods were compared. ATR measurements showed higher content of collagen then CD measurements, but there are also similarities between these two methods. Samples with the lowest and the highest contents of collagen are same for both methods. It proves that we can compare samples with different collagen content to each other but we cannot determine exact collagen content by connecting these two methods. Difference in collagen contents were caused by inaccurate deconvolution of amide I peak mentioned before. It proves that ATR spectroscopy is much easier and faster but can be used just for approximate results. Results obtained with CD method are more accurate but need consistent preparation of samples and setting of spectrophotometer. Optimized sample preparation method will be used for next planned investigations and measurements with bovine collagen.

7 REFERENCES

[1] LIU, Yaowen, Donghui MA, Yihao WANG a Wen QIN. A comparative study of the properties and self-aggregation behavior of collagens from the scales and skin of grass carp (Ctenopharyngodon idella). *International Journal of Biological Macromolecules*. 2018, **106**, 516-522. DOI: 10.1016/j.ijbiomac.2017.08.044. ISSN 01418130

[2] ZHANG, Qiang, Qianqian WANG, Shun LV, Jianfeng LU, Shaotong JIANG, Joe M. REGENSTEIN a Lin LIN. Comparison of collagen and gelatin extracted from the skins of Nile tilapia (Oreochromis niloticus) and channel catfish (Ictalurus punctatus). *Food Bioscience*. 2016, **13**, 41-48. DOI: 10.1016/j.fbio.2015.12.005. ISSN 22124292.

[3] TZIVELEKA, Leto-Aikaterini, Efstathia IOANNOU, Dimitris TSIOURVAS, Panagiotis BERILLIS, Evangelia FOUFA a Vassilios ROUSSIS. Collagen from the Marine Sponges Axinella cannabina and Suberites carnosus: Isolation and Morphological, Biochemical, and Biophysical Characterization. *Marine Drugs*. 2017, **15**(6), 152-. DOI: 10.3390/md15060152. ISSN 1660-3397.

[4] ABRAHAM, Leah C., Erin ZUENA, Bernardo PEREZ-RAMIREZ a David L. KAPLAN. Guide to collagen characterization for biomaterial studies. Journal of Biomedical Materials Research Part B: Applied Biomaterials. 2008, 87B(1), 264-285. DOI: 10.1002/jbm.b.31078. ISSN 15524973.

[5] KURODA, Reiko, Takunori HARADA a Yohji SHINDO. A solid-state dedicated circular dichroism spectrophotometer: Development and application. *Review of Scientific Instruments* [online]. American Institute of Physics, 2001, **72**(10), 3802-3810 [cit. 2018-05-04]. DOI: 10.1063/1.1400157. ISSN 0034-6748.

[6] LEE, Chi H., Anuj SINGLA a Yugyung LEE. Biomedical applications of collagen. *International Journal of Pharmaceutics*. 2001, **221**(1-2), 1-22. DOI: 10.1016/S0378-5173(01)00691-3. ISSN 03785173.

[7] FRIESS, Wolfgang. Collagen – biomaterial for drug delivery. European Journal of Pharmaceutics and Biopharmaceutics. 1998, 45(2), 113-136. DOI: 10.1016/S0939-6411(98)00017-4. ISSN 09396411.

[8] GÓMEZ-GUILLÉN, M.C., B. GIMÉNEZ, M.E. LÓPEZ-CABALLERO a M.P. MONTERO. Functional and bioactive properties of collagen and gelatin from alternative sources: A review. Food Hydrocolloids. 2011, 25(8), 1813-1827. DOI: 10.1016/j.foodhyd.2011.02.007. ISSN 0268005x.

[9] TRAUB, Wolfie a Karl A. PIEZ. The Chemistry and Structure of Collagen. *Science Direct*. Elsevier, 1971, 1971, (25), 243-352. Advances in Protein Chemistry. DOI: 10.1016/S0065-3233(08)60281-8. ISBN 9780120342259.

[10] Kolagen - vlastnosti, modifikace a aplikace. Brno: Vysoké učení technické v Brně, 2000, 94(6). ISSN ISSN 1213-7103.

[11] BRODSKY, Barbara a John A.M. RAMSHAW. The collagen triple-helix structure. Matrix Biology. 1997, 15(8-9), 545-554. DOI: 10.1016/S0945-053X(97)90030-5. ISSN 0945053X.

[12] XU, Yujia. Thermal Stability of Collagen Triple Helix. *Biothermodynamics, Part B*. Elsevier, 2009, 2009, **466**, 211-232. Methods in Enzymology. DOI: 10.1016/S0076-6879(09)66009-2. ISBN 9780123747761. ISSN 0916572X.

[13] DÖLZ, R. a E. HEIDEMANN. Influence of different tripeptides on the stability of the collagen triple helix. I. Analysis of the collagen sequence and identification of typical tripeptides. Biopolymers. 1986, 25(6), 1069-1080. DOI: 10.1002/bip.360250607. ISSN 00063525.

[14] WANG, Jing, Xinli PEI, Haiying LIU a Dan ZHOU. Extraction and characterization of acid-soluble and pepsin-soluble collagen from skin of loach (Misgurnus anguillicaudatus). International Journal of Biological Macromolecules. 2018, 106, 544-550. DOI: 10.1016/j.ijbiomac.2017.08.046. ISSN 01418130.

[15] HARRINGTON, William F. a Peter H. VON HIPPEL. The Structure Of Collagen And Gelatin. *Advances in Protein Chemistry*. Elsevier, 1962, 1962, (16), 1-138. Advances in Protein Chemistry. DOI: 10.1016/S0065-3233(08)60028-5. ISBN 9780120342167.

[16] YAKIMETS, Iryna, Nikolaus WELLNER, Andrew C. SMITH, Reginald H. WILSON, Imad FARHAT a John MITCHELL. Mechanical properties with respect to water content of gelatin films in glassy state. Polymer. 2005, 46(26), 12577-12585. DOI: 10.1016/j.polymer.2005.10.090. ISSN 00323861.

[17] KELLY, Sharon M., Thomas J. JESS a Nicholas C. PRICE. How to study proteins by circular dichroism. Biochimica et Biophysica Acta (BBA) - Proteins and Proteomics. 2005, 1751(2), 119-139. DOI: 10.1016/j.bbapap.2005.06.005. ISSN 15709639.

[18] KOZLOV, P.V. a G.I. BURDYGINA. The structure and properties of solid gelatin and the principles of their modification. Polymer. 1983, 24(6), 651-666. DOI: 10.1016/0032-3861(83)90001-0. ISSN 00323861.

[19] YAO, Han, Evelien WYNENDAELE, Xiaolong XU, Anne KOSGEI a Bart DE SPIEGELEER. Circular dichroism in functional quality evaluation of medicines. Journal of Pharmaceutical and Biomedical Analysis. 2018, 147, 50-64. DOI: 10.1016/j.jpba.2017.08.031. ISSN 07317085.

[20] BARROW, Colin J., Akikazu YASUDA, Peter T.M. KENNY a Michael G. ZAGORSKI. Solution conformations and aggregational properties of synthetic amyloid β-peptides of Alzheimer's disease. Journal of Molecular Biology. 1992, 225(4), 1075-1093. DOI: 10.1016/0022-2836(92)90106-T. ISSN 00222836.

[21] Synchrotron Radiation Circular Dichroism. In: *Aarhus University* [online]. Aarhus University Nordre Ringgade, Denmark: Aarhus University, 2014 [cit. 2018-03-20]. Dostupné z: http://www.isa.au.dk/facilities/astrid2/beamlines/AU-cd/AU-CD_3.asp

[22] D. FASMAN., Gerald. *Circular dichroism and the conformational analysis of biomolecules*. New York, N.Y: Springer, 2010. ISBN 978-144-1932-495.

[23] STUART, Barbara. Infrared spectroscopy: fundamentals and applications. Hoboken, NJ: J. Wiley, 2004. ISBN 04-708-5427-8.

[24] ALI, Ali Muhammed Moula, Soottawat BENJAKUL a Hideki KISHIMURA. MOLECULAR CHARACTERISTICS OF ACID AND PEPSIN SOLUBLE COLLAGENS FROM THE SCALES OF GOLDEN CARP (PROBARBUS JULLIENI). *Emirates Journal of Food and Agriculture*. 2017, **29**(6), 450-. DOI: 10.9755/ejfa.2016-09-1316. ISSN 2079-0538.

[25] ALI, Ali Muhammed Moula, Hideki KISHIMURA a Soottawat BENJAKUL. Extraction efficiency and characteristics of acid and pepsin soluble collagens from the skin of golden carp (Probarbus Jullieni) as affected by ultrasonication. *Process Biochemistry*. 2018, **66**, 237-244. DOI: 10.1016/j.procbio.2018.01.003. ISSN 13595113.

[26] CHUAYCHAN, Sira, Soottawat BENJAKUL a Hideki KISHIMURA. Characteristics of acid- and pepsin-soluble collagens from scale of seabass (Lates calcarifer). *LWT - Food Science and Technology*. 2015, **63**(1), 71-76. DOI: 10.1016/j.lwt.2015.03.002. ISSN 00236438.

[27] TIFANY, M. Lois a S. KRIMM. Effwct of temperature on the circular dichroism spectra of polypeptides in the extended state. *Biopolymers*. 1972, **11**(11), 2309-2316. DOI: 10.1002/bip.1972.360111109. ISSN 0006-3525.

[28] LIANG, Qiufang, Lin WANG, Weihong SUN, Zhenbin WANG, Junmin XU a Haile MA. Isolation and characterization of collagen from the cartilage of Amur sturgeon (Acipenser schrenckii). *Process Biochemistry*. 2014, **49**(2), 318-323. DOI: 10.1016/j.procbio.2013.12.003. ISSN 13595113.

[29] ZOU, Ye, Li WANG, Panpan CAI, et al. Effect of ultrasound assisted extraction on the physicochemical and functional properties of collagen from soft-shelled turtle calipash. International Journal of Biological Macromolecules. 2017, 105, 1602-1610. DOI: 10.1016/j.ijbiomac.2017.03.011. ISSN 01418130.

[30] YU, Zhi-Long, Wei-Cai ZENG, Wen-Hua ZHANG, Xue-Pin LIAO a Bi SHI. Effect of ultrasound on the activity and conformation of α-amylase, papain and pepsin. *Ultrasonics Sonochemistry*. 2014, **21**(3), 930-936. DOI: 10.1016/j.ultsonch.2013.11.002. ISSN 13504177.

[31] IKOMA, Toshiyuki, Hisatoshi KOBAYASHI, Junzo TANAKA, Dominic WALSH a Stephen MANN. Physical properties of type I collagen extracted from fish scales of Pagrus major and Oreochromis niloticas. *International Journal of Biological Macromolecules*. 2003, **32**(3-5), 199-204. DOI: 10.1016/S0141-8130(03)00054-0. ISSN 01418130.

[32] WOOD, Ashley, Masahiro OGAWA, Ralph J. PORTIER, Mark SCHEXNAYDER, Mark SHIRLEY a Jack N. LOSSO. Biochemical properties of alligator (Alligator mississippiensis) bone collagen. *Comparative Biochemistry and Physiology Part B: Biochemistry and Molecular Biology*. 2008, **151**(3), 246-249. DOI: 10.1016/j.cbpb.2008.05.015. ISSN 10964959.

[33] BARTH, Andreas. Infrared spectroscopy of proteins. *Biochimica et Biophysica Acta (BBA) - Bioenergetics*. 2007, **1767**(9), 1073-1101. DOI: 10.1016/j.bbabio.2007.06.004. ISSN 00052728.

[34] GLASSFORD, Stefanie E., Bernadette BYRNE a Sergei G. KAZARIAN. Recent applications of ATR FTIR spectroscopy and imaging to proteins. Biochimica et Biophysica Acta (BBA) - Proteins and Proteomics. 2013, 1834(12), Pages 2849-2858. DOI: 10.1016/j.bbapap.2013.07.015. ISBN 10.1016/j.bbapap.2013.07.015.

[35] TAMM, LUKAS K. a SUREN A. TATULIAN. Infrared spectroscopy of proteins and peptides in lipid bilayers. *Quarterly Reviews of Biophysics*. 1997, **30**(4), 365-429. DOI: 10.1017/S0033583597003375. ISSN 00335835.

[36] ATAKA, Kenichi a Joachim HEBERLE. Biochemical applications of surface-enhanced infrared absorption spectroscopy. *Analytical and Bioanalytical Chemistry*. 2007, **388**(1), 47-54. DOI: 10.1007/s00216-006-1071-4. ISSN 1618-2642.

[37] OBERG, Keith A. a Anthony L. FINK. A New Attenuated Total Reflectance Fourier Transform Infrared Spectroscopy Method for the Study of Proteins in Solution. *Analytical Biochemistry*. 1998, **256**(1), 92-106. DOI: 10.1006/abio.1997.2486. ISSN 00032697.

[38] KRIMM, Samuel a Jagdeesh BANDEKAR. Vibrational Spectroscopy and Conformation of Peptides, Polypeptides, and Proteins. *Advances in Protein Chemistry Volume 38*. Elsevier, 1986, 1986, , 181-364. Advances in Protein Chemistry. DOI: 10.1016/S0065-3233(08)60528-8. ISBN 9780120342389.

[39] WANG, Yingli, Kaixia XU, Yani LI a Qianjin FENG. Fourier transform infrared spectroscopy analysis of the active components in serum of rats treated with Zuogui Pill. *Journal of Traditional Chinese Medical Sciences*. 2015, **2**(4), 264-269. DOI: 10.1016/j.jtcms.2016.01.006. ISSN 20957548.

[40] NEVSKAYA, N. A. a Yu. N. CHIRGADZE. Infrared spectra and resonance interactions of amide-I and II vibrations of α-helix. *Biopolymers*. 1976, **15**(4), 607-648. DOI: 10.1002/bip.1976.360150404. ISSN 0006-3525.

[41] TORII, Hajime a Mitsuo TASUMI. Model calculations on the amide-I infrared bands of globular proteins. The Journal of Chemical Physics. 1992, 96(5), 3379-3387. DOI: 10.1063/1.461939. ISSN 0021-9606.

[42] REISDORF,, William C. a Samuel KRIMM. Infrared Amide I‘ Band of the Coiled Coil †. *Biochemistry*. 1996, **35**(5), 1383-1386. DOI: 10.1021/bi951589v. ISSN 0006-2960.

[43] HEIMBURG, Thomas, Juergen SCHUENEMANN, Klaus WEBER a Norbert GEISLER. Specific Recognition of Coiled Coils by Infrared Spectroscopy: Analysis of the Three Structural Domains of Type III Intermediate Filament Proteins. *Biochemistry*. 1996, **35**(5), 1375-1382. DOI: 10.1021/bi9515883. ISSN 0006-2960.

[44] VENYAMINOV, S. Yu. a N. N. KALNIN. Quantitative IR spectrophotometry of peptide compounds in water (H2O) solutions. II. Amide absorption bands of polypeptides and fibrous proteins in α-, β-, and random coil conformations. *Biopolymers*. 1990, **30**, 13-14. DOI: 10.1002/bip.360301310. ISBN 10.1002/bip.360301310.

[45] CHIRGADZE, Yu. N. a E. V. BRAZHNIKOV. Intensities and other spectral parameters of infrared amide bands of polypeptides in the α-helical form. *Biopolymers*. 1974, **13**(9), 1701-1712. DOI: 10.1002/bip.1974.360130902. ISSN 0006-3525.

[46] MARTINEZ, Gary a Glenn MILLHAUSER. FTIR Spectroscopy of Alanine-Based Peptides: Assignment of the Amide I′ Modes for Random Coil and Helix. *Journal of Structural Biology*. 1995, **114**(1), 23-27. DOI: 10.1006/jsbi.1995.1002. ISSN 10478477.

[47] MUKHERJEE, Smita, Pramit CHOWDHURY a Feng GAI. Infrared Study of the Effect of Hydration on the Amide I Band and Aggregation Properties of Helical Peptides. *The Journal of Physical Chemistry B*. 2007, **111**(17), 4596-4602. DOI: 10.1021/jp0689060. ISSN 1520-6106.

[48] Intermolecular Interaction Effects in the Amide I Vibrations of β Polypeptides. National Academy of Sciences, 1976, **69**(no. 10). ISSN 0027-8424.

[49] BARTH, Andreas a Christian ZSCHERP. What vibrations tell about proteins. *Quarterly Reviews of Biophysics*. 2002, **35**(4), 369-430. DOI: 10.1017/S0033583502003815. ISSN 00335835.

[50] SCHWEITZER-STENNER, Reinhard. Advances in vibrational spectroscopy as a sensitive probe of peptide and protein structure. *Vibrational Spectroscopy*. 2006, **42**(1), 98-117. DOI: 10.1016/j.vibspec.2006.01.004. ISSN 09242031.

[51] ABE, Yasuaki a S. KRIMM. Normal vibrations of crystalline polyglycine I. *Biopolymers*. 1972, **11**(9), 1817-1839. DOI: 10.1002/bip.1972.360110905. ISSN 0006-3525.

[52] OBERG, Keith A., Jean-Marie RUYSSCHAERT a Erik GOORMAGHTIGH. The optimization of protein secondary structure determination with infrared and circular dichroism spectra. *European Journal of Biochemistry*. 2004, **271**(14), 2937-2948. DOI: 10.1111/j.1432-1033.2004.04220.x. ISSN 00142956.

[53] SINTHUSAMRAN, Sittichoke, Soottawat BENJAKUL a Hideki KISHIMURA. Comparative study on molecular characteristics of acid soluble collagens from skin and swim bladder of seabass (Lates calcarifer). *Food Chemistry*. 2013, **138**(4), 2435-2441. DOI: 10.1016/j.foodchem.2012.11.136. ISSN 03088146.

[54] CHEN, Junde, Long LI, Ruizao YI, Nuohua XU, Ran GAO a Bihong HONG. Extraction and characterization of acid-soluble collagen from scales and skin of tilapia (Oreochromis niloticus). *LWT - Food Science and Technology*. 2016, **66**, 453-459. DOI: 10.1016/j.lwt.2015.10.070. ISSN 00236438.

[55] KITTIPHATTANABAWON, Phanat, Soottawat BENJAKUL, Wonnop VISESSANGUAN, Takashi NAGAI a Munehiko TANAKA. Characterisation of acid-soluble collagen from skin and bone of bigeye snapper (Priacanthus tayenus). *Food Chemistry*. 2005, **89**(3), 363-372. DOI: 10.1016/j.foodchem.2004.02.042. ISSN 03088146.

[56] DOYLE, Barbara Brodsky, E. G. BENDIT a Elkan R. BLOUT. Infrared spectroscopy of collagen and collagen-like polypeptides. Biopolymers. 1975, 14(5), 937-957. DOI: 10.1002/bip.1975.360140505. ISSN 0006-3525.

[57] MUYONGA, J.H., C.G.B. COLE a K.G. DUODU. Characterisation of acid soluble collagen from skins of young and adult Nile perch (Lates niloticus). *Food Chemistry*. 2004, **85**(1), 81-89. DOI: 10.1016/j.foodchem.2003.06.006. ISSN 03088146.

[58] SUREWICZ, Witold K. a Henry H. MANTSCH. New insight into protein secondary structure from resolution-enhanced infrared spectra. Biochimica et Biophysica Acta (BBA) - Protein Structure and Molecular Enzymology. 1988, 952, 115-130. DOI: 10.1016/0167-4838(88)90107-0. ISSN 01674838.

[59] ZANABONI, Giuseppe, Antonio ROSSI, Angèle M.Tina ONANA a Ruggero TENNI. Stability and networks of hydrogen bonds of the collagen triple helical structure: influence of pH and chaotropic nature of three anions. *Matrix Biology*. 2000, **19**(6), 511-520. DOI: 10.1016/S0945-053X(00)00096-2. ISSN 0945053X.

[60] KITTIPHATTANABAWON, Phanat, Soottawat BENJAKUL, Wonnop VISESSANGUAN a Fereidoon SHAHIDI. Isolation and properties of acid- and pepsin-soluble collagen from the skin of blacktip shark (Carcharhinus limbatus). *European Food Research and Technology*. 2010, **230**(3), 475-483. DOI: 10.1007/s00217-009-1191-0. ISSN 1438-2377.

[61] SAMPATH KUMAR, N.S. a R.A. NAZEER. Characterization of Acid and Pepsin Soluble Collagen from the Skin of Horse Mackerels (Magalaspis cordyla) and Croaker (Otolithes ruber). *International Journal of Food Properties*. 2013, **16**(3), 613-621. DOI: 10.1080/10942912.2011.557796. ISSN 1094-2912.

[62] GUZZI PLEPIS, Ana Maria De, Gilberto GOISSIS a Dilip K. DAS-GUPTA. Dielectric and pyroelectric characterization of anionic and native collagen. *Polymer Engineering and Science*. 1996, **36**(24), 2932-2938. DOI: 10.1002/pen.10694. ISBN 10.1002/pen.10694.

[63] DUAN, Rui, Junjie ZHANG, Xiuqiao DU, Xingcun YAO a Kunihiko KONNO. Properties of collagen from skin, scale and bone of carp (Cyprinus carpio). *Food Chemistry*. 2009, **112**(3), 702-706. DOI: 10.1016/j.foodchem.2008.06.020. ISSN 03088146.

[64] NAGAI, T. Isolation of collagen from fish waste material — skin, bone and fins. *Food Chemistry*. 2000, **68**(3), 277-281. DOI: 10.1016/S0308-8146(99)00188-0. ISSN 03088146.

[65] ZHANG, Junjie a Rui DUAN. Characterisation of acid-soluble and pepsin-solubilised collagen from frog (Rana nigromaculata) skin. *International Journal of Biological Macromolecules*. 2017, **101**, 638-642. DOI: 10.1016/j.ijbiomac.2017.03.143. ISSN 01418130.

[66] FENNEMA, Owen R. *Food chemistry*. 3rd ed. New York: Marcel Dekker, 1996. Food science and technology (Marcel Dekker, Inc.), v. 76. ISBN 08-247-9346-3.

[67] SATO, Kaori, Tetsuya EBIHARA, Eijiro ADACHI, Seiichi KAWASHIMA, Shunji HATTORI a Shinkichi IRIE. Possible Involvement of Aminotelopeptide in Self-assembly and Thermal Stability of Collagen I as Revealed by Its Removal with Proteases. *Journal of Biological Chemistry*. 2000, **275**(33), 25870-25875. DOI: 10.1074/jbc.M003700200. ISSN 0021-9258.

[68] SUN, Leilei, Bafang LI, Wenkui SONG, Leilei SI a Hu HOU. Characterization of Pacific cod (Gadus macrocephalus) skin collagen and fabrication of collagen sponge as a good biocompatible biomedical material. *Process Biochemistry*. 2017, **63**, 229-235. DOI: 10.1016/j.procbio.2017.08.003. ISSN 13595113.

[69] SENARATNE, L.S., Pyo-Jam PARK a Se-Kwon KIM. Isolation and characterization of collagen from brown backed toadfish (Lagocephalus gloveri) skin. *Bioresource Technology*. 2006, **97**(2), 191-197. DOI: 10.1016/j.biortech.2005.02.024. ISSN 09608524.

[70] ZHANG, Qiang, Qianqian WANG, Shun LV, Jianfeng LU, Shaotong JIANG, Joe M. REGENSTEIN a Lin LIN. Comparison of collagen and gelatin extracted from the skins of Nile tilapia (Oreochromis niloticus) and channel catfish (Ictalurus punctatus). *Food Bioscience*. 2016, **13**, 41-48. DOI: 10.1016/j.fbio.2015.12.005. ISSN 22124292.

[71] LI, Zhong-Rui, Bin WANG, Chang-feng CHI, Qi-Hong ZHANG, Yan-dan GONG, Jia-Jia TANG, Hong-yu LUO a Guo-fang DING. Isolation and characterization of acid soluble collagens and pepsin soluble collagens from the skin and bone of Spanish mackerel (Scomberomorous niphonius). *Food Hydrocolloids*. 2013, **31**(1), 103-113. DOI: 10.1016/j.foodhyd.2012.10.001. ISSN 0268005X.

[72] LIU, H.Y., J. HAN a S.D. GUO. Characteristics of the gelatin extracted from Channel Catfish (Ictalurus Punctatus) head bones. LWT - Food Science and Technology. 2009, 42(2), 540-544. DOI: 10.1016/j.lwt.2008.07.013. ISSN 00236438.

[73] MUYONGA, J.H, C.G.B COLE a K.G DUODU. Fourier transform infrared (FTIR) spectroscopic study of acid soluble collagen and gelatin from skins and bones of young and adult Nile perch (Lates niloticus). *Food Chemistry*. 2004, **86**(3), 325-332. DOI: 10.1016/j.foodchem.2003.09.038. ISSN 03088146.

[74] BYLER, D. Michael a Heino SUSI. Examination of the secondary structure of proteins by deconvolved FTIR spectra. *Biopolymers*. 1986, **25**(3), 469-487. DOI: 10.1002/bip.360250307. ISSN 0006-3525.

[75] FRIESS, W. Basic thermoanalytical studies of insoluble collagen matrices. Biomaterials [online]. 1996, 17(23), 2289-2294 [cit. 2018-04-08]. DOI: 10.1016/0142-9612(96)00047-6. ISSN 01429612.

[76] PRYSTUPA, D.A. a A.M. DONALD. Infrared study of gelatin conformations in the gel and sol states. *Polymer Gels and Networks*. 1996, **4**(2), 87-110. DOI: 10.1016/0966-7822(96)00003-2. ISSN 09667822.

[77] PAYNE, K. J. a A. VEIS. Fourier transform ir spectroscopy of collagen and gelatin solutions: Deconvolution of the amide I band for conformational studies. *Biopolymers*. 1988, **27**(11), 1749-1760. DOI: 10.1002/bip.360271105. ISSN 0006-3525.

[78] GEORGE, Anne a Arthur VEIS. FTIRS in water demonstrates that collagen monomers undergo a conformational transition prior to thermal self-assembly in vitro. *Biochemistry*. 2002, **30**(9), 2372-2377. DOI: 10.1021/bi00223a011. ISSN 0006-2960.

[79] RENUGOPALAKRISHNAN, V., G. CHANDRAKASAN, S. MOORE, T. B. HUTSON, C. V. BERNEY a Rajendra S. BHATNAGAR. Bound water in collagen: evidence from Fourier transform infrared and Fourier transform infrared photoacoustic spectroscopic study. *Macromolecules*. 1989, **22**(10), 4121-4124. DOI: 10.1021/ma00200a054. ISSN 0024-9297.

8 ABBREVIATIONS

AB – gelatin extracted from adult fish bones
Ala – alanine
AS – gelatin extracted from adult fish skins
ASC – acid soluble collagen
ATR – Attenuated total reflectance spectroscopy
Avg – average
CD – circular dichroism
EDTA – ethylenediaminetetraacetic acid
FTIR – Fourier transform infrared spectroscopy
GAA – glacial acetic acid
Gly – glycine
HCl – hydrochloric acid
H_2O – water
H_2O_2 – hydrogen peroxide
H_2SO_4 – sulphuric acid
HT – Jasco labeling of voltage of photomultiplier
Hyp – hydroxyproline
IR – infrared spectroscopy
LCP – left-handed circularly polarized
NaOH – sodium hydroxide
Pro – proline
PSC – pepsin soluble collagen
RPM – rotations per minute
RCP – right-handed circularly polarized
SSC – salt soluble collagen
TDC – transition dipole coupling
UASC – acid soluble collagen in ultrasound
UPSC – pepsin soluble collagenin ultrasound
UV – ultra violent light
YB – gelatin extracted from young fish bones
YS – gelatin extracted from young fish skins

9 LIST OF FIGURES

10 LIST OF TABLES